



# The heuristic vulnerability model: fragility curves for masonry buildings

Sergio Lagomarsino<sup>1</sup> · Serena Cattari<sup>1</sup> · Daria Ottonelli<sup>1</sup>

Received: 12 July 2020 / Accepted: 12 February 2021  
© The Author(s) 2021

## Abstract

In the framework of seismic risk analyses at large scale, among the available methods for the vulnerability assessment the empirical and expert elicitation based ones still represent one of most widely used options. In fact, despite some drawbacks, they benefit of a direct correlation to the actual seismic behaviour of buildings and they are easy to handle also on huge stocks of buildings. Within this context, the paper illustrates a macroseismic vulnerability model for unreinforced masonry existing buildings that starts from the original proposal of Lagomarsino and Giovinazzi (Bull Earthquake Eng 4(4):445–463, 2006) and has further developed in recent years. The method may be classified as heuristic, in the sense that: (a) it is based on the expertise that is implicit in the European Macroseismic Scale (EMS98), with fuzzy assumptions on the binomial damage distribution; (b) it is calibrated on the observed damage in Italy, available in the database Da.D.O. developed by the Italian Department of Civil Protection (DPC). This approach guarantees a fairly well fitting with actual damage but, at the same time, ensures physically consistent results for both low and high values of the seismic intensity (for which observed data are incomplete or lacking). Moreover, the method provides a coherent distribution between the different damage levels. The valuable data in Da.D.O. allowed significant improvements of the method than its original version. The model has been recently applied in the context of ReLUIIS project, funded by the DPC to support the development of Italian Risk Maps. To this aim, the vulnerability model has been applied for deriving fragility curves. This step requires to introduce a correlation law between the Macroseismic Intensity (adopted for the calibration of the model from a wide set of real damage data) and the Peak Ground Acceleration (at present, one of most used instrumental intensity measures); this conversion further increases the potential of the macroseismic method. As presented in the paper, the first applications of the model have produced plausible and consistent results at national scale, both in terms of damage scenarios and total risk (economic loss, consequences to people).

**Keywords** Macroseismic vulnerability model · Fragility curves · Vulnerability index · Mean damage grade · Calibration by observed damage

---

✉ Sergio Lagomarsino  
sergio.lagomarsino@unige.it

<sup>1</sup> Department of Civil, Chemical and Environmental Engineering, University of Genoa, Genova, Italy

## 1 Introduction

The aim of seismic risk analyses is to evaluate the expected losses in a given area (e.g. a city or a wider region), taking into consideration the exposed buildings (e.g. the residential building stock or a portfolio of specific buildings, like hospitals or schools) and the related contents (e.g. movable objects) and the consequences to involved people.

The quantification of the risk is intrinsically probabilistic because earthquake is a random action and the performance of buildings, as well as losses and consequence to people, are affected by uncertainties. For each type of consequence, the mean expected loss (either annual or referred to another reference time) is obtained by the convolution integral, according to the Performance-Based Earthquake Engineering (PBEE) methodology developed at the Pacific Earthquake Engineering Research (PEER) (Cornell and Krawinkler 2000; Porter 2003; Moehle and Deierlein 2004). In this case the result is an unconditioned scenario, because it is not related to a specific seismic event but it considers the effect of all possible earthquakes, with different intensity and probability of occurrence, following the Probabilistic Seismic Hazard Assessment (PSHA) in the area.

Sometimes it is useful to evaluate the seismic risk scenario for a single specific seismic intensity in each point of the study area. It is the case of the event-based risk calculation, which considers a deterministic hazard scenario given by the attenuation of the reference seismic intensity from the epicenter and gives a picture of the corresponding possible damage scenario; this is useful, for example, to support the emergency planning. Another example is the conditioned scenario that considers in each location the effect of the earthquake expected with a given return period. In both these cases the risk assessment is probabilistic, because of the uncertainty in the fragility and the consequence models.

The fragility curves give the relation between the intensity measure (IM) and the damage measure (DM) to structural and non-structural elements, representative of the global behavior of the building. Sometimes the fragility curves are defined as a function of an Engineering Demand Parameter (EDP), correlated to the IM through a structural model and selected because well correlated to the damage variable. The damage can be measured by a continuous variable but usually reference is made to a discrete damage measure, through overall damage grades (D), analogous to the ones used in the post-earthquake damage observation (i.e. the 5 damage of the European Macroseismic Scale, EMS98, Grunthal 1998). The name given to these damage grades is slightly different in the literature, due to the qualitative/fuzzy definition; moreover, a correspondence with the limit states adopted for the performance-based assessment and usually introduced in Standards (e.g. ASCE/SEI 41-13 2014, Eurocode 8–3 CEN 2005) is also possible. Table 1 gives a general picture of these definitions. In the following, reference is made to the damage grades according to the EMS98 ( $D_k$ ,  $k=1, \dots, 5$ ).

**Table 1** Damage measures adopted for the fragility

DM	EMS98 damage grades ( $D_k$ )	Other definition (Hazus)	Limit states (EC8)
1	Negligible to slight	Slight	Fully operational
2	Moderate	Moderate	Damage limitation
3	Substantial to heavy	Extensive	Significant damage
4	Very heavy	Complete	Near collapse
5	Destruction	–	–

The fragility function of a given  $D_k$  gives the probability that such a damage is reached or exceeded as a function of the IM (or the related EDP). The lognormal cumulative function is worldwide used to this aim and is defined by only two parameters: the median value  $IM_{Dk}$  of the intensity measure that induces a damage equal or greater than  $D_k$  and the corresponding dispersion  $\beta_{Dk}$ , which depends on the involved uncertainties (e.g. HAZUS 1999). First of all, a significant dispersion is associated to the record-to-record variability, because the selected IM is not by itself sufficient to identify exactly whether the damage  $D_k$  is achieved or not. Moreover, when fragility functions of a homogeneous group of buildings are derived via a numerical way through an archetype building, the variability in the material properties and structural details of the actual buildings increases the dispersion. In seismic risk analyses, buildings are classified according to a taxonomy, in order to group together buildings with a similar behavior; therefore, for each building class more than one archetype building is necessary to represent the seismic performance, and this increases the dispersion of the corresponding fragility curve.

The loss, in terms of different possible Decision Variables (DV), is then evaluated by consequence functions, by using as input the result of the fragility analysis. Uncertainties are present also in this last step of the seismic risk analysis.

This paper is focused on the derivation of fragility functions for unreinforced masonry (URM) buildings, to be used for the seismic risk assessment at large scale, and in particular for whole Italy. Different methods can be adopted which may be classified as follows (Rossetto et al. 2014; Lagomarsino and Cattari 2014): (1) empirical; (2) mechanical-based (analytical or numerical); (3) expertise-based (heuristic); (4) hybrid.

Empirical fragility functions are derived directly from the post-earthquake damage data (Del Gaudio et al. 2017, 2019a, 2019b; Rosti et al. 2019; Bertelli et al. 2018) and, at a first glance, it is assumed they represent the actual behavior of the real buildings that formed the building class. Mechanical-based methods require the idealization of the building class through one or more archetype buildings, to be investigated through numerical models (usually nonlinear dynamic analyses, through: incremental dynamic analysis—IDA, cloud method, multiple-stripe analysis—MSA) or analytical simplified formulations, which depends on few relevant parameters (available in the inventory for the whole building stock), for example: Bernardini et al. (1990), D'Ayala et al. (1997), Calvi (1999), Glaiser and Pihno (2003), Restrepo and Magenes (2004), D'Ayala (2005), Borzi et al. (2008), Molina et al. (2009), Oropeza et al. (2010), Lagomarsino and Cattari (2013), Rota et al. (2010), Erberik (2008), Gehl et al. (2013), Donà et al. (2019). Expertise-based methods seems to be not supported by objective data (observational and/or mechanical) but define the fragility in a coherent way, passing through the different damage grades and comparing different building types (e.g. Jaiswal et al. 2011; Lagomarsino and Giovinazzi 2006). In addition, hybrid approaches combine the three above-mentioned methods. Table 2 summarizes pros and cons of the different methods.

In this paper, a new method for the derivation of fragility functions for residential building stocks is proposed (Sect. 3). It is based on the macroseismic method (Lagomarsino and Giovinazzi 2006; Bernardini et al. 2011), which is an expertise-based method derived from the European Macroseismic Scale EMS98 (Grunthal 1998) and whose basic principles are recalled at Sect. 2. The EMS98 implicitly contains a relation between damage and intensity for a set of vulnerability classes (from A to F), which are associated to different buildings types, both in masonry and reinforced concrete (RC). The IM originally used by the macroseismic method is obviously the macroseismic Intensity ( $I$ ) but a correlation with Peak Ground Acceleration (PGA) was proposed too and then lognormal fragility functions were

**Table 2** Pros and cons of the different methods for the derivation of fragility functions

Method	IM	PROS	CONS
Empirical	I-PGA	Supported by actual observed data	(1) Incompleteness and lack of data; (2) Reliability of IM associated to observations; (3) Extension of functions out of the range of available data
Mechanical-based	PGA- $S_a(T_p)$ -Housner Intensity—mean spectral values	(1) Use of physically-consistent IM; (2) Soil-dependence of fragility functions	1) Validation and calibration of models; (2) Selection of representative archetypes
Expertise-based	I-PGA	Coherence: (1) for low and high values of IM; (2) Comparing building types	(1) Big dispersion, due to the rough classification; (2) Need of validation and calibration

then derived in Lagomarsino and Cattari (2014). However, before the further developments presented in this paper, a robust validation of the method by real data was missing.

The method here proposed is based on a heuristic approach, in the sense that it is a non-rigorous procedure that allows to predict a result which must then be validated by observed damage; despite that, it preserves the valuable information of the original expertise-based macroseismic method. The vulnerability model keeps the original structure of the macroseismic model proposed in Lagomarsino and Giovinazzi (2006): the vulnerability of a group of buildings is defined by a vulnerability index, from which expertise-based fragility functions are analytically obtained. However, one of the most relevant novelty in this paper is that the value of the vulnerability index associated to any specific building type (classified by material, age and number of stories) is obtained by a calibration with observed data. The latter was made by using Da.D.O.—Database of Observed Damage (Dolce et al. 2017, 2019), which collects the observed damage after the main earthquakes in the last 40 years in Italy, from Friuli 1976. In particular, information from Irpinia (1980) and L'Aquila (2009) earthquakes are detailed and almost complete, because they contain comprehensive information on both the building characteristics (age, number of floors) and the damage induced in areas hit by different macroseismic intensities. The method was derived, so far, only for URM buildings but it would be easily extended to RC ones.

Finally, the method was implemented in the IRMA platform (Sect. 4), developed by Eucentre (Borzi et al. 2018; Faravelli et al. 2019) for the evaluation of the seismic risk to residential buildings in Italy through the ISTAT census data (2001); in fact, the latter contains information that allows the same classification into sub-types of buildings adopted for the calibration of fragility curves with Da.D.O.. The results are presented in the paper and highlight the reliability of the model, by a comparison in terms of different losses and consequences (total expected economic loss, number of victims), both in terms of unconditional scenarios and in the simulation of specific occurred earthquakes (Sect. 5). Moreover, the available data on the L'Aquila 2009 earthquake were also used to validate the model (Sect. 5.1).

## 2 The macroseismic method

The macroseismic intensity  $I$  cannot be considered a physically consistent measure of the seismic shaking because it implicitly contains the vulnerability of buildings in the area. This inconsistency was acceptable at the origin of macroseismic scales (e.g. Mercalli 1900), when only masonry buildings were present and the vulnerability of the built environment was almost uniform, but it became a significant drawback after the birth of new building types (RC buildings) and even more with the introduction of the aseismic design. In order to avoid this drawback, the EMS98 was introduced (Gruntal 1998). As known, it considers six different vulnerability classes, from Class A, the one with the worst behavior, to Class F, representative of seismically designed modern buildings; for each class, a different relation between macroseismic intensity and damage is established. Damage is described by the aforementioned 5 damage grades (Table 1), which may be ascribed to a building through a visual survey after an earthquake by the observation of the severity and extent of damage in structural and nonstructural elements.

The identification of the damage grade during the macroseismic survey is subjective, even if surveyors should be trained, because is based on some reference sketches and qualitative descriptions. The aim of EMS98 is to assign an objective value to the macroseismic

intensity in an urban area, regardless of the type of buildings; this is obtained through the table of Fig. 1, which quantifies the percentage of buildings subjected to a given damage in qualitative terms (according to a fuzzy definition). The heuristic nature of this model may be expressed by the following considerations:

- For each vulnerability class (buildings of similar seismic behavior), the increase of one degree in the macroseismic intensity induces an increase of one damage grade.
- For each intensity degree, passing from one to the following vulnerability class the induced damage is reduced by one grade.

Regardless of the macroseismic survey, the damage assessment procedure adopted in Italy (Baggio et al. 2002) requires filling in the AeDES form in which damage levels are ascribed to different elements (vertical/horizontal, structural/nonstructural), thus allowing a more detailed and objective evaluation. However, the AeDES form does not require to end up with a synthetic measure, representative of the damage grade of the whole building and the way to combine all these pieces of information is still an open issue (Rota et al 2008; Dolce et al. 2017; Del Gaudio et al. 2017). The arbitrariness of this empirical approach is not conceptually far from the one related to the identification of damage grades from mechanical models, where nonlinear static (pushover) or dynamic analyses firstly provide a picture of force/displacement demand in each structural element but then it is necessary to identify a synthetic EDP and the correspondent performance thresholds to fix the attainment of the damage grade at global scale (Lagomarsino and Cattari 2015).

According to the EMS98, the vulnerability class collects all the buildings that present a similar seismic performance, in the sense of a given relation between intensity and damage. EMS98 provides a table (Fig. 2) in which a possible correspondence between building types (in masonry or reinforced concrete) and vulnerability classes is established. It is evident that, in the case of URM buildings, the masonry type (rubble stone, adobe, massive stone, etc.) is the main parameter to characterize the vulnerability, while, in the case of RC buildings, the structural system (frames, walls) and the level of earthquake resistant design are the crucial parameters. Anyhow, this table highlights two relevant aspects:

- Buildings of the same type might behave differently, due to other specific features that are not univocally associated to the masonry type. Therefore, for each building type there is a most likely vulnerability class (the majority of this kind of build-

<i>I</i>	D1 negligible to slight	D2 moderate	D3 substantial to heavy	D4 very heavy	D5 destruction
5	Few A/B				
6	Many A/B, Few C	Few A/B			
7		Many B, Few C	Many A, Few B	Few A	
8		Many C, Few D	Many B, Few C	Many A, Few B	Few A
9		Many D, Few E	Many C, Few D	Many B, Few C	Many A, Few B
10		Many E, Few F	Many D, Few E	Many C, Few D	Most A, Many B, Few C
11		Many F	Many E, Few F	Most C, Many D, Few E	Most B, Many C, Few D
12					All A/B, Most D/E/F, Nearly All C

Fig. 1 Correlation between intensity and damage for the vulnerability classes of EMS98 (adapted from Grunthal 1998)

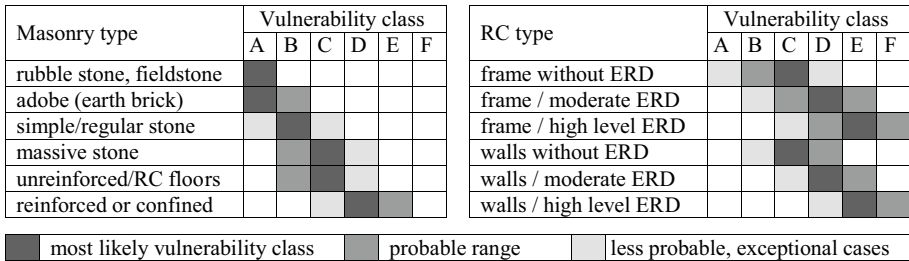


**Fig. 2** Building type matrix of EMS98 and correlation with the vulnerability classes (adapted from Grunthal 1998)

ings belong to this class) but many buildings of this type might behave according to another class, and sometimes there are exceptional cases of a small percentage (but no negligible at territorial level) of buildings that belong to another class.

- In the same vulnerability class, there are buildings of different type (masonry types apparently very different, but also RC buildings). This means that after an earthquake you can observe, in a given town, the same damage degree in buildings that are very different from the typological point of view.

Regarding the first aspect, it is worth noting that rubble stone masonry buildings always shows a high vulnerability (Class A), while in the case of massive stone buildings or modern URM with RC floors the most probable behavior is that of Class C, but many buildings have a lower performance (Class B) and there are also some very good buildings (Class D). With reference to the second issue, it is evident the seismic behavior of Class B may be found in simple or manufactured stone buildings, but also in the best adobe buildings and in the worst massive stone buildings and modern URM with RC floors.

It is evident that within a specific building type the best or worst behavior is due to other building features, like the number of stories, the type of horizontal diaphragms, the regularity in plan and elevation, the structural details (e.g. the quality of connections between masonry walls). These features are not explicitly considered in EMS98 and are at the base of the taxonomy of a residential building stock. According to the available information at territorial scale, a classification of the building stock into sub-types is possible, and the related vulnerability may be defined within the general framework of EMS98, by selecting the proper vulnerability class or even specifying in a more detailed way.

An overly detailed subdivision into sub-types is not useful, both because often the inventory does not contain all the information and the vulnerability would be, at the end, not so different indeed. It is worth noting that the dispersion of the seismic behavior of buildings belonging to the same EMS98 type (Fig. 2) may be very high, because of the presence of buildings of different vulnerability classes, and splitting the building type into sub-types leads to a reduction of the dispersion. However, the dispersion is not reduced too much because, within any sub-type, even if specified by all possible taxonomy features, buildings of different architectural configurations and other characteristics not considered by the taxonomy live together.

Lagomarsino and Giovinazzi (2006) have proposed the macroseismic vulnerability method, directly derived from the EMS98, for any vulnerability class, through the following assumptions:

- The transformation of the qualitative definition (few, many, most,...) in EMS98 (Fig. 1) of the amount of buildings which suffered a given damage for a given intensity into quantitative percentages: this was done by using the fuzzy set theory.
- The completion of the Damage Probability Matrix (DPM), which gives for any intensity the histogram of damage grades, was made by assuming the binomial probability distribution that turned out to be coherent with the damage observation (Braga et al. 1982).

The binomial distribution gives the probability of attainment a given damage grade  $D_k$  ( $k=0, 1, \dots, 5$ ) by one continuous free parameter only, the mean damage grade  $\mu_D$  ( $0 \leq \mu_D \leq 5$ ):

$$p_k = \frac{5!}{k!(5-k)!} \left(\frac{\mu_D}{5}\right)^k \left(1 - \frac{\mu_D}{5}\right)^{5-k} \tag{1}$$

$$\mu_D = \sum_{k=1}^5 p_k k \tag{2}$$

The mean damage grade increases with the intensity according to the macroseismic vulnerability curve:

$$\mu_D = 2.5 \left[ 1 + \tanh\left(\frac{I + 6.25V - 13.1}{2.3}\right) \right] \tag{3}$$

where  $I$  is the macroseismic intensity and  $V$  is the vulnerability index that assumes, for the EMS98 vulnerability classes, the values in Table 3 in order to fit the values of the binomial DPM obtained by the fuzzy set theory (Bernardini et al. 2011). In particular, the range of the values with the maximum plausibility is indicated, together with the white values, defined as the central value within the range of the class according to the fuzzy set theory (Klir and Yuan 1995). Figure 3 shows the macroseismic vulnerability curves for the EMS98 vulnerability classes, evaluated from the values of vulnerability indexes summarized in Table 3.

Once the vulnerability curve of a building type is known by the representative vulnerability index  $V$ , it is possible to derive numerical fragility curves in terms of intensity:

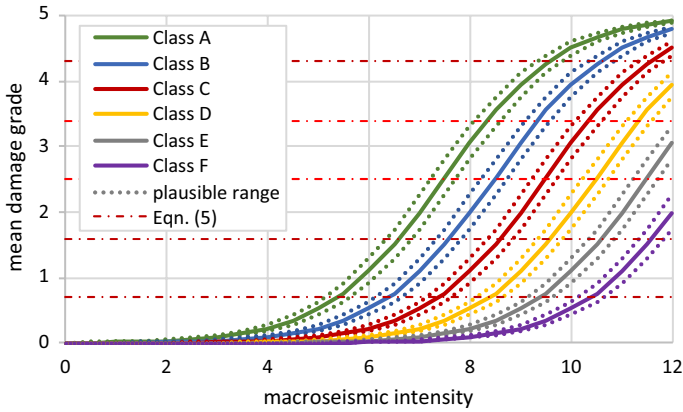
$$p_{V,k}(I) = P(DM \geq D_k | I) = \sum_{i=k}^5 p_i \tag{4}$$

Figure 4 shows the fragility curves in terms of intensity derived by the macroseismic vulnerability method, in the case of vulnerability Class B (white value) for the different damage grades (Fig. 4a) or in the case of damage grade  $D_2$  for the six EMS98 vulnerability classes (Fig. 4b).

**Table 3** White values of the vulnerability index for the EMS98 vulnerability classes

Vulnerability class	A	B	C	D	E	F
V—white value	0.9	0.74	0.58	0.42	0.26	0.10
V—plausible interval	0.86–0.94	0.70–0.78	0.54–0.62	0.38–0.46	0.22–0.30	0.06–0.14





**Fig. 3** Macroseismic vulnerability curves derived for the EMS98 vulnerability classes (white and plausible intervals of the vulnerability index  $V$ )

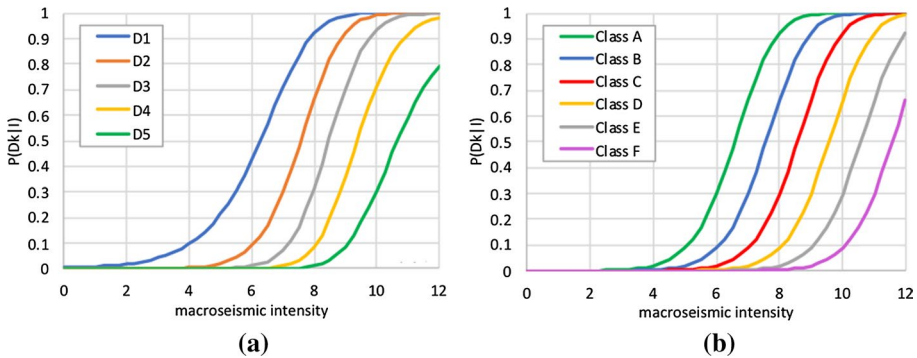


**Fig. 4** Fragility curves in intensity for: **a** all damage grades for Class A; **b** damage grade 2 of all vulnerability classes

It is worth noting that, as the macroseismic intensity is a discrete measure of the earthquake, the definition of continuous macroseismic vulnerability curves and their related fragility curves is theoretically non-consistent. However, in the macroseismic survey after an earthquake, the use of intermediate values of the macroseismic intensity is quite common (e.g. 7.5 or, more correctly, 7/8). Indeed, the seismic intensity is by its nature continuous and the definition of the macroseismic intensity as a discrete measure is only operative.

The fragility curves, expressed analytically by Eq. (4), have a shape very different by the widely used lognormal fragility functions, just because the intensity is not a physical measure of the earthquake shaking, but an empirical measure limited to  $I=12$ . In order to get the median intensity value of the fragility curve, it is necessary to derive from the binomial distribution the mean damage grade for which the probability of each damage grade  $k$  is equal to 0.5. The five values are well fitted by the following equation (these values are indicated in Fig. 3, by horizontal dashed-dotted lines):

$$\mu_{D,k} = 0.9k - 0.2 \tag{5}$$

Then, it is easy to obtain the median intensity value of the fragility curve, by using Eqs. (3) and (5):

$$I_k = 13.1 - 6.25V + 2.3 \operatorname{atanh}(0.36k - 1.08) \quad (6)$$

The presented formulation is very effective and clear for the risk analysis of residential building stocks in a town or a wide region, as testified by many applications of the method after its proposal (e.g. Castillo et al. 2011; Cherif et al. 2017; Cosenza et al. 2018; Lestuzzi et al. 2016; Maio et al. 2018; Neves et al. 2012). Buildings should be grouped into homogeneous sub-types, on the base of the available information. The EMS98 provides rough directions for a classification which only considers the material type and the relation between intensity and damage is very disperse because it should be related to a wide variability of building performance at European level. Within a specific region it is expected a better-defined behavior, also considering the availability of other information on the structural features. Therefore, the analytical formulation of the macroseismic vulnerability model allows to ascribe to each sub-type a specific value of the vulnerability index  $V$ , through which the macroseismic vulnerability curve and the correspondent fragility curves are obtained. For each masonry type, a range of possible values of the vulnerability index  $V$  are obtained directly from the EMS98, which states the large variety of seismic performance (even belonging to different vulnerability classes) within a group of buildings characterized only by the masonry type. When more information is available from the inventory, such as number of stories, age or other structural details, building sub-types may be identified and the corresponding vulnerability may be differentiated by adding to the mean value of the masonry type the vulnerability modifier  $\Delta V$  (positive or negative), which may be derived by expert judgment, observed damage or analytical/numerical models. It is evident that the more the sub-type is well-defined, through a detailed taxonomy, the lower is the expected dispersion of the building performance. However, it is assumed that even in the case of a detailed assessment/inventory the damage histogram is never less disperse than that of the binomial distribution, which may be considered a sort of lower bound for a sub-set of buildings; the latter is because of architectural variability that cannot be considered at territorial scale, when the information is statistical and not specific to the single building.

### 3 The heuristic vulnerability model

The macroseismic vulnerability method, briefly described in the previous section, was converted in terms of  $PGA$  by assuming different  $I$ - $PGA$  correlations taken from literature (Faccioli and Cauzzi 2006; Murphy and O'Brien 1977) and comparing the results with those from mechanical-based models (Lagomarsino and Cattari 2014). However, a systematic validation of the method with observed data is still lacking. This validation and further developments of the method were made within the ambit of a research project promoted by the Italian Civil Protection Department (DPC) and that involved the ReLUI consortium and EUCENTRE (Dolce and Prota 2020), aimed to develop the Italian risk assessment for the residential building stock (Italian Civil Protection Department 2018). Many research groups were involved and different approaches for the development of fragility curves were adopted, all of them calibrated and validated through a comprehensive database of observed damage (Da.D.O.), which collects the survey forms collected after the main earthquakes occurred in Italy in the last 40 years (Dolce et al. 2017, 2019).

The inventory of the building stock used for the risk assessment comes from the census of the population made in 2001 (ISTAT 2001), within which for any building a form was filled, with information on: structural material; age of construction; number of stories. Data are available in aggregated form for each municipality, in terms of number of buildings, number of flats, built surface, together with the number of inhabitants.

In the following, the new heuristic vulnerability model is illustrated. As aforementioned, it is derived from the macroseismic one through a calibration/validation taking profit of the observed damage in Da.D.O. and considering the characteristics of the IRMA platform (Borzi et al. 2018), which was used for the risk calculation.

### 3.1 Processing of observed damage data

Da.D.O. ([http://egeos.eucentre.it/danno\\_osservato/web/danno\\_osservato](http://egeos.eucentre.it/danno_osservato/web/danno_osservato)) is a web-gis platform that collects the observed damage to residential buildings after nine different earthquakes in Italy: Friuli (1976), Irpinia (1980), Abruzzo (1984), Umbria-Marche (1997), Pollino (1998), Molise e Puglia (2002), Emilia (2003), L'Aquila (2009), Emilia (2012). Table 4 shows the number of buildings (distinguishing masonry and RC) that are present in the database, together with the range of the macroseismic intensity for which damage data are available.

The survey form and procedure were not the same all along more than 40 years, so a first critical issue is how to convert the available damage information into the EMS98 damage grade (from  $D_0$  to  $D_5$ ). This conversion was made within the Da.D.O. platform according to specific rules described in Dolce et al. (2019), but it is also possible to process the original data according to alternative proposals.

To each damage record, referred to a specific building, the seismic input should be associated. For vulnerability models that considers the macroseismic intensity, like the one described in Sect. 2, the intensity assigned to that location by the macroseismic survey was assumed. Other models require a physically-based intensity measure, like the PGA. Shake maps derived from recorded accelerations in specific points in the area should be used; however, it is worth noting that reliable shake maps are available only for the last earthquakes, thanks to the increasing presence of many accelerometric stations in the area (<http://itaca.mi.ingv.it>, Accelerometric National Network—RAN).

**Table 4** Characteristics of the available extracted from Da.D.O. (Dolce et al. 2019)

Earthquake	# of blds*	RC	Masonry	Intensity	Towns
Friuli (1976)	41,852	469	29,641	4.5–9	400
Irpinia (1980)	33,220	3576	26,335	5–9	1248
Abruzzo (1984)	46,200	2130	39,078	4–8	888
Umbria-Marche (1997)	34,873	2296	29,512	4–9	737
Pollino (1998)	16,689	1508	13,887	5–7	33
Molise e Puglia (2002)	23,623	2374	19,031	4–8.5	684
Emilia (2003)	994	–	906	5–7	95
L'Aquila (2009)	73,793	12,755	51,438	5–9	137
Emilia (2012)	22,489	1991	18,194	5–7.5	47

\*Buildings to which the macroseismic intensity is known

The use of observed damage requires a preliminary assessment of the quality of data, both in terms of completeness and potential errors. First of all, it is evident that for a robust calibration/validation of fragility curves it is necessary to have a large number of data, distributed in locations that suffered different seismic intensities, up to those that induce a significant damage level. For this reason, some of the earthquakes in Table 4, although interesting, are not useful for a systematic calibration of the heuristic vulnerability model. For example, considering the main earthquakes, the Friuli (1976), Umbria-Marche (1997) and Emilia (2012) earthquakes present lack of data in the area far from the epicenter. The check of completeness was made by ISTAT census, by comparing the available damage records with the number of buildings in each location. It emerged that only Irpinia (1980) and L'Aquila (2009) have a robust rate of completeness, which slightly decreases moving far from the epicenter; thus, the estimated number of lacking damage records was used to complete the damage histogram in each location, by assuming that those buildings were not damaged. Indeed, this is consistent with the fact that far from the epicenter the survey was made only to the damaged buildings under specific request of the owner.

Table 5 shows the number of buildings with available damage data for different seismic intensities. For the case of L'Aquila earthquake, the completeness of the damage survey was checked by comparing the number of buildings expected from ISTAT census (2001); it emerges that for the highest values of the macroseismic intensity (greater than 6) the damage survey was complete, while far from the epicenter only buildings that suffered some damage have been assessed. It is worth noting that for intensity greater than 8 the number of surveyed buildings is even more than what is expected from ISTAT inventory; the reasons may be related to the identification of buildings during the AeDES damage survey, which, in particular in the aggregates of historical centres, leads to a more detailed subdivision with respect to what was done during the ISTAT census. Therefore, in the case of L'Aquila earthquake, the missed buildings in the area far from the epicenter are considered without damage. Regarding the Irpinia earthquake, not having an ISTAT database prior to 1980, reference was made to the 1991 database. The latter has no information about the number of buildings, but it contains the number of dwellings for each district and consequently municipality. This parameter has been adopted for the analysis of the completeness of the database. From the comparison between the number of dwellings from Da.D.O. and ISTAT database emerged a good consistency, since in each municipality in Da.D.O. the number of dwelling surveyed is greater than the 80% of the ISTAT ones, even in the case of low intensity.

The damage assessment was made with different forms in the two considered seismic events. The Irpinia form classified the damage into 8 levels, while the AeDES form (Baggio et al. 2002) was used after the L'Aquila earthquake. Regarding the conversion from damage information to the EMS98 damage degree, slightly different assumptions were made in this paper with respect to the Da.D.O. proposals.

**Table 5** Number of surveyed buildings and expected total number in the different areas

Earthquake	Database	# Of blds	Macroseismic intensity							
			<6	6	6.5	7	7.5	8	8.5	9
Irpinia (1908)	Da.D.O	33,220	1971	2255	1437	11,944	—	11,553	—	4060
L'Aquila (2009)	Da.D.O	73,793	13,887	27,081	3609	3950	4871	780	12,183	7432
	ISTAT	114,825	60,611	31,227	3012	3287	3919	726	7262	4781

**Table 6** Correlation between damage score after Irpinia earthquake and the assumed EMS98 damage degree

Irpinia (1980)	Damage level							
	1	2	3	4	5	6	7	8
Da.D.O	0	1	1	2	2	3	4	5
This paper	0	0.7	1.4	2.1	2.9	3.6	4.3	5

**Table 7** Weights  $w_i$  of the different types of elements, depending of the survey detail

Survey	Vertical	Horizontal	Stairs	Roof	Infills
Complete survey	0.6	0.2	0	0.2	0
Survey from outside	0.8	0	0	0.2	0

In the case of Irpinia earthquake, a direct correspondence was established in Da.D.O. among the damage levels (see Table 6), while for the calibration of the macroseismic method a continuous damage level was evaluated, by simply assuming that the eight levels of the Irpinia form represented a gradually homogeneous increase of damage.

This choice was made to not introduce a bias in the correlation, because the calibration of the method considers a continuous damage measure, the mean damage grade  $\mu_D$ , representative of the damage distribution of buildings in areas that suffered the same macroseismic intensity.

Differently, the AeDES form adopted for L'Aquila earthquake contains, in Sect. 4, information on the damage to primary and secondary structural elements, classified as: (1) vertical, (2) horizontal, (3) stairs, (4) roof, and (5) infills. Then for each one, the local damage is measured by three levels (Light—D1; Moderate to heavy—D2/D3; Very heavy—D4/D5) and the extension within the building is indicated (A—spread on more than 2/3; B—between 1/3 and 2/3; C—< 1/3). Therefore, an overall damage grade is not defined. The one in Da.D.O. is based only on the damage occurred in vertical structural elements, by assuming proper conversion rules as a function of its extension. However, this approach tends to overestimate the damage grade that would be assigned by applying the EMS98 scale and does not consider other important elements. Thus, in the present paper, a weighted average of damage in all elements is evaluated, by considering the diffusion and assuming proper weights for the different elements. In particular, more importance to the damage to vertical structural elements, roof and also to horizontal floors (when the survey was made also inside the building, information that is present in Da.D.O.) has been assumed. The damage grade is then calculated by the following relation:

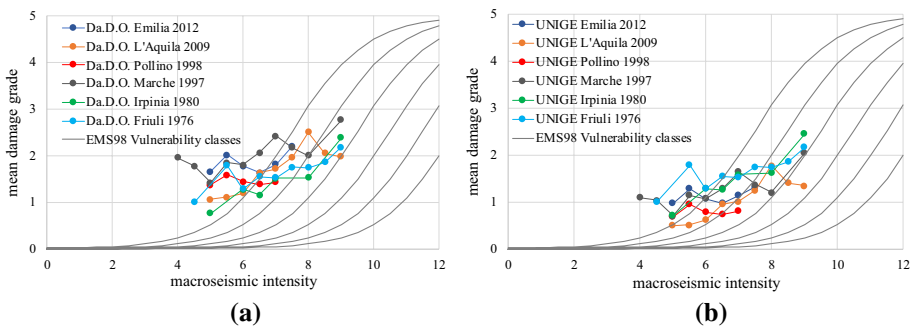
$$D_{AeDES} = \sum_{i=1}^5 w_i \sum_{j=1}^3 (2j - 1)v_{i,j} \tag{7}$$

where  $w_i$  is the weight given to the 5 different elements (Table 7),  $v_{i,j}$  is percentage of the elements of type  $i$  in which it was observed the damage  $j$ . According to the extension previously indicated,  $v_{i,j}$  was tentatively assumed equal to: 1 (A); 2/3 (B), 1/3 (C), 0 (when no option is indicated). It is evident that  $\sum_{j=1}^3 v_{i,j}$  must be less than or equal to one (if it is less than one it means that some elements were not damaged); when it results greater than 1 but values in the form are compatible with the intervals, the values of  $v_{i,j}$  were normalized.

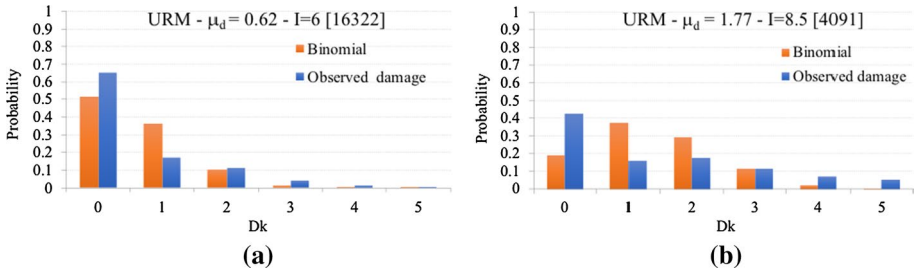
Moreover, specific checks were made to single out clear errors and the most plausible actual damage was defined. By using Eq. (7) the damage level results a continuous value between 0 to 5, which may be discretized by assuming, for example, the damage equal to 1 if  $0.5 < D_{AeDES} < 1.5$ . However, analogously to the Irpinia earthquake, the definition of a discrete damage level to any single building is not necessary for the calibration of the method.

Figure 5 shows the increase of the mean damage grade with the macroseismic intensity for the damage data from all the available earthquakes, according to both: the Da.D.O. (a) and the proposed damage measure (b). The latter presents, as expected, lower values and a slightly more regular and similar trend for all earthquakes. It is evident how the mean damage grade remains almost constant for intensity lower than 6: this is because the lack of buildings in that locations, which are probably undamaged. Their presence would correctly reduce the mean damage grade, but in the case of L'Aquila earthquake it has been avoided an arbitrary completion of the database (therefore, they were neglected in the calibration). These observational macroseismic vulnerability curves follow the typical trend of the ones derived from EMS98 for the vulnerability classes (Fig. 3); however, it is worth noting that masonry buildings are here considered altogether while a better trend is observed by grouping buildings according to homogenous types (see Sect. 3.2).

In particular, focusing the attention to Irpinia and L'Aquila earthquakes data, masonry buildings seem to be globally a bit less vulnerable in the case of L'Aquila. It is useful specifying that curves are referred to all masonry buildings, without a classification in sub-types, but the same trend would be observed in the different ages of construction. It is worth noting that the increase of damage with intensity is lower than that foreseen by the macroseismic method (Eq. 3), because in low intensity areas the damage is overestimated for different reasons: (i) the database is not complete (because in the municipalities far from the epicenter undamaged buildings were not surveyed); (ii) when damage is low there is an attitude of surveyors to record any light damage, often neglected if the damage is higher, and sometimes the surveyors prefer to take precautions. A strange trend may be observed in the case of L'Aquila for the higher intensity values (8.5–9); these data are referred to the epicentral area where most of the buildings are from L'Aquila town and are constituted by the good quality palaces of the historical centre (expected to be better than the poor masonry buildings in the surrounding areas) and by a bigger percentage of modern buildings.



**Fig. 5** Empirical macroseismic vulnerability curves, compared with the observed damage evaluated by considering: **a** Da.D.O. damage level; **b** proposed definition of the damage level



**Fig. 6** Observational and binomial damage distribution for masonry buildings after L'Aquila earthquake, in areas that suffered intensity 6 (a) and 8.5 (b); the number of building is indicated in square brackets

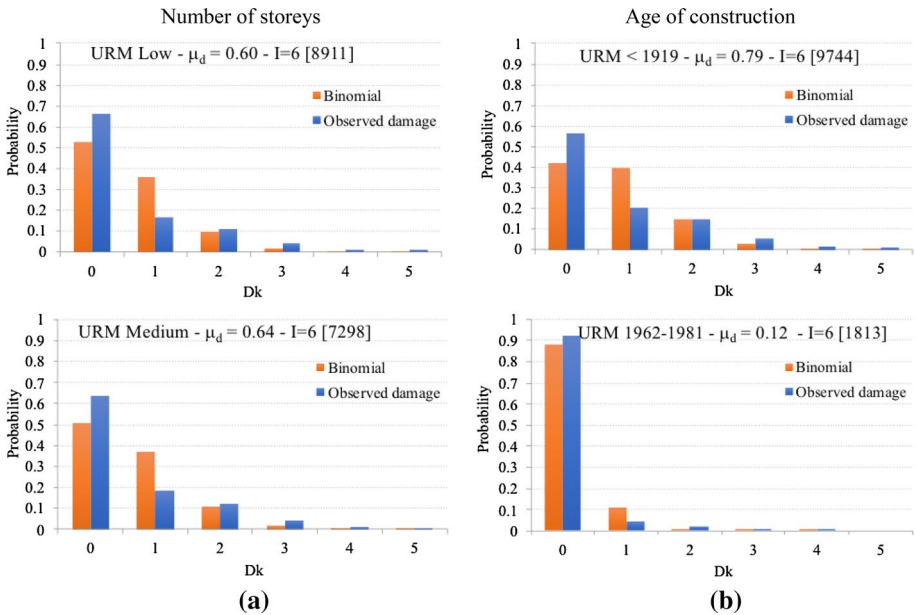


**Fig. 7** Observational and binomial damage distribution for some ISTAT sub-types of masonry buildings after L'Aquila earthquake, for intensity 6 (the number of building is indicated in square brackets): **a** influence of the height of the building; **b** influence of the age of construction

In order to check the validity of binomial damage distribution, the damage histograms have been evaluated for different intensity values and aggregation of building types. Focusing to L'Aquila earthquake, Fig. 6 shows the observed damage histogram of all masonry buildings in areas with macroseismic intensity 6 and 8, compared with the binomial distribution evaluated for the same mean damage grade. It is worth noting that the observed damage presents a bigger dispersion with respect to that of the binomial distribution: this occurs because very different buildings are treated altogether. Figure 7 shows that by dividing masonry buildings into sub-types, by age and number of stories, the dispersion is significantly reduced and the binomial distribution fits quite well the observed damage. This confirms the relevance of these parameters for the classification



of masonry buildings. It is worth noting that while the age influences significantly the vulnerability (Fig. 7b), the height of the building is not particularly relevant (the mean damage grade is almost constant).

### 3.2 Calibration of the macroseismic vulnerability method for ISTAT masonry building sub-types

The macroseismic vulnerability method is represented by Eq. (3) as a function of one free parameter, the vulnerability index  $V$ ; then, the fragility curves in macroseismic intensity may be derived from Eqns. (5) and (6). The calibration with observed data for Italian masonry buildings was made by using Da.D.O. and considering only the Irpinia (1980) and L'Aquila (2009) earthquakes, as motivated by the good level of completeness and good distribution in terms of intensity degree as documented in Sect. 3.1. For these two earthquakes, an accurate check of reliability of the information in Da.D.O. was made; in particular, in the case of L'Aquila earthquake, due to missing data in the low intensity areas, only locations with intensity greater or equal to 6 have been considered.

The damage database was treated by grouping all buildings subjected to the same macroseismic intensity and splitting them into sub-types of masonry buildings, according to the information in ISTAT census (ISTAT 2001):

- Number of stories: L (low-rise, 1–2 stories), M (mid-rise, from 3 to 5) and H (high-rise, > 5).
- Age of construction: A1 (< 1919), A2 (1919–1945), A3 (1946–1961), A4 (1962–1981) and A5 (> 1981); actually, ISTAT data are more detailed, but this classification was made in order to have a statistically relevant number of buildings in each sub-set.

Tables 8 and 9 show the number of available data with the different intensity degrees, for the Irpinia and L'Aquila earthquake respectively. It is worth noting that in the case of Irpinia earthquake the intervals related to the age of construction are a bit different and, obviously, the A5 is not present. It emerges that the number of buildings reduces for the highest intensity degree, because the epicentral area is smaller. Moreover, very few data are available for high-rise buildings; as they are not statistically significant, the model was not calibrated for high-rise buildings and their vulnerability was assumed by expert judgement through the comparison with that of the low and mid-rise buildings.

**Table 8** Number of buildings for which damage data are available after Irpinia earthquake

Intensity	A1 (< 1900)			A2 (1900–1943)			A3 (1944–1961)			A4 (1962–1980)		
	L	M	H	L	M	H	L	M	H	L	M	H
5	619	102	0	150	15	0	191	32	0	187	42	0
6	552	266	0	302	89	0	227	39	0	250	65	0
6.5	416	144	0	144	31	0	92	9	0	175	13	0
7	2954	248	2	2082	143	0	909	69	0	2086	140	1
8	3350	754	4	1900	298	1	718	93	0	1038	152	1
9	1086	93	3	904	17	0	399	10	0	432	14	0
Total	8977	1607	9	5482	593	1	2536	252	0	4168	426	2



**Table 9** Number of buildings for which damage data are available after L'Aquila earthquake

Intensity	A1 (<1919)			A2 (1919–1945)			A3 (1946–1961)			A4 (1962–1981)			A5 (>1981)		
	L	M	H	L	M	H	L	M	H	L	M	H	L	M	H
5	1111	1798	12	304	250	0	144	100	0	178	99	10	59	73	17
5.5	1200	1813	9	419	440	0	216	146	0	215	164	1	85	81	0
6	5003	4664	14	1373	942	2	885	408	0	1024	781	0	408	335	0
6.5	743	686	1	115	94	0	43	21	0	106	69	0	34	58	0
7	871	799	1	118	100	0	88	69	0	133	120	0	45	35	0
7.5	1045	662	0	238	127	0	134	68	0	178	184	0	99	79	0
8	130	73	0	62	33	0	24	3	0	49	32	0	18	11	0
8.5	871	857	0	371	210	1	281	188	1	501	350	0	185	126	5
9	881	672	0	223	130	0	188	95	1	357	279	0	148	126	0
total	11,855	12,024	37	3223	2326	3	2003	1098	2	2741	2078	11	1081	924	22

For each sub-type, the empirical points of the macroseismic vulnerability curve were obtained by collecting all values of the damage level for the same macroseismic intensity and evaluating the mean damage grade (Fig. 8). The trend looks similar to that of Fig. 3 but the increase of the mean damage grade with the macroseismic intensity (slope of the curve) is not the same in all the sub-types. It is worth noting that EMS98 gives a general framework of the vulnerability of all building types, with the aim of giving the maximum objectivity to the macroseismic intensity survey; in other words, the EMS98 scale is the result of an expert

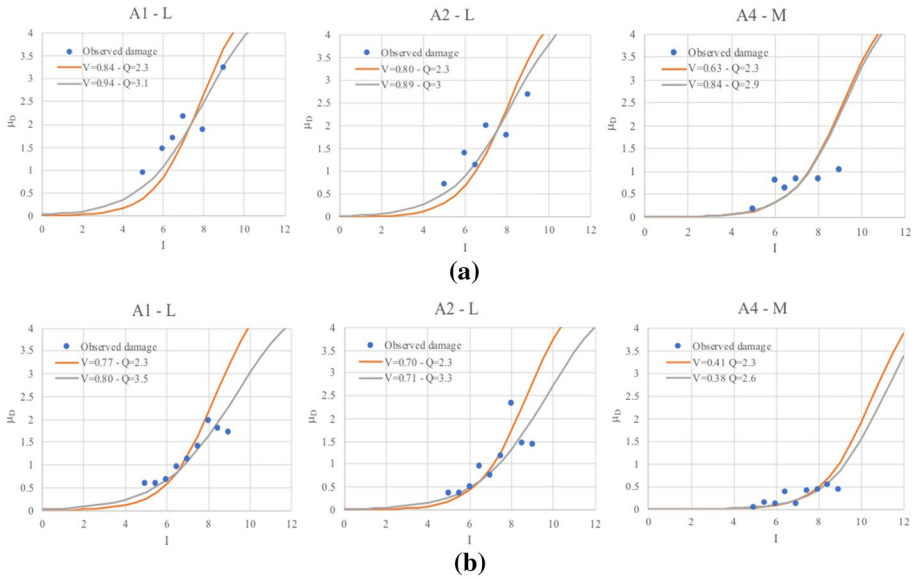


**Fig. 8** Derivation of macroseismic vulnerability curves from observed damage: **a** Irpinia; **b** L'Aquila. The best fit by using the original macroseismic model is in orange color, while the vulnerability  $V$  and ductility  $Q$  indexes of the new proposed formulation are in grey color

elicitation that cannot consider the different behavior of any building type. With the aim of a calibration with observed damage, a second free parameter, the ductility index  $Q$ , is introduced in the macroseismic vulnerability curve:

$$\mu_D = 2.5 \left[ 1 + \tanh \left( \frac{I + 6.25V - Q - 10.8}{Q} \right) \right] \tag{8}$$

The ductility index  $Q$  determines the slope of these curves, and the value  $Q=2.3$  is strictly related to the assumption of the EMS98, for which in each vulnerability class the increment of the intensity by one degree determines an increase of one in the damage distribution. Higher values of  $Q$  correspond to a slope decrease, which means that it is necessary to increase the intensity of more than one degree in order to have the increase of one in the damage distribution (ductile behavior). Figure 8 shows both the best fit of  $V$  by using the original macroseismic model (with  $Q=2.3$ ) and the vulnerability  $V$  and ductility  $Q$  indexes of the new proposed formulation.

The fitted values were represented as a function of the building age, both for low and mid-rise buildings, distinguishing the Irpinia and L'Aquila earthquake (Fig. 9). Regarding the vulnerability index  $V$ , as expected, it increases with the age of the buildings, while a less clear influence of the building height is observed. In particular, in the case of L'Aquila earthquake, mid-rise buildings turn out to be less vulnerable than the low-rise ones: this may be due to the better quality of mid-rise buildings with respect to the poor and less important low-rise ones, mainly located out of the urban areas. The same trend is observed in Irpinia, but only for the sub-types before 1945. The vulnerability results a bit higher in the case of Irpinia earthquake (Fig. 9a); this result may be coherent with the distinctive features of masonry buildings in the two areas, but also by the uncertainties related to the attribution of damage levels (from the different survey forms adopted in the two earthquakes) and of the macroseismic intensity.

Another interesting outcome is that the ductility index  $Q$  is not constant for the different ages and a correlation with the vulnerability index  $V$  is evident:  $Q$  decreases when  $V$  decreases (that is for modern engineered buildings). In order to limit the number of free parameters of the model, the following correlation has been obtained:

$$Q = 0.9 + 2.8V \geq 1.8 \tag{9}$$

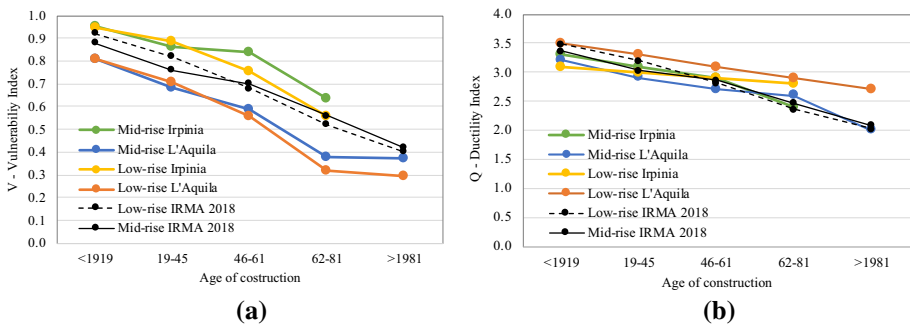


**Fig. 9** Calibration of the vulnerability  $V$  (a) and ductility  $Q$  (b) indexes with observed damage data. Values assumed for the scenario at National scale are in black color (see Sect. 4.1)

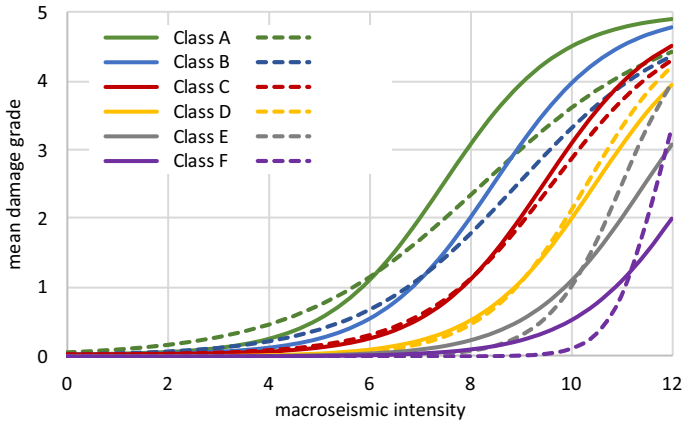


**Fig. 10** Comparison between EMS98 (continuous lines) and calibrated (dashed lines) macroseismic vulnerability curves for the Classes from A to F

**Table 10** White values and plausible interval of  $V$  for the vulnerability classes in the new model

Vulnerability Class	A	B	C	D	E	F
$V$ —white value	1	0.8	0.6	0.4	0.2	0.0
$V$ —plausible interval	0.95–1.05	0.75–0.85	0.55–0.65	0.35–0.45	0.15–0.25	–0.05–0.05

where a lower bound for  $Q$  is assumed, compatible with the values fitted by the observed data. Therefore, the macroseismic vulnerability curve is thus modified:

$$\mu_D = \begin{cases} 2.5 \left[ 1 + \tanh \left( \frac{I+3.45V-11.7}{0.9+2.8V} \right) \right] & \text{for } V \geq 0.32 \\ 2.5 \left[ 1 + \tanh \left( \frac{I+6.25V-12.6}{1.8} \right) \right] & \text{for } V < 0.32 \end{cases} \quad (10)$$

The original (see Sect. 2) and the new calibrated macroseismic vulnerability curves are compared in Fig. 10; it is worth noting that in order to represent as much as possible the EMS98 vulnerability classes, the values of  $V$  (Table 10) are slightly modified with respect to the original ones (Table 3), in order to be compatible with the EMS98 for mean damage grades up to 2 (those encountered most frequently for medium intensity earthquakes and also in the case of strong events in the wide area surrounding the epicentral one).

It is worth noting that the value  $Q=2.3$ , implicitly derivable from EMS98, seems to be correct for modern masonry buildings (Classes C and D), while for the traditional ones a bigger value is observed. The bigger ductility observed for ancient masonry buildings may be due to the fact that, even if modern buildings have a bigger shear strength their ductility is lower, due to the brittle behavior of hollow blocks and to the weak-piers & strong-spandrels collapse mechanism, which may be induced by the presence of RC tie beams. Moreover, it should be considered that these curves represent the performance of a set of buildings and the bigger ductility should be interpreted as a wider variability of the

architectural configurations of the buildings in the set, typical of ancient buildings more than engineered modern ones.

Finally, the values of the vulnerability index  $V$  derived from the calibration with the observed data range between 1 and 0.4, values which are characteristic of vulnerability classes from A to D, being fully coherent with the EMS98 (Fig. 2); indeed, very modern masonry buildings (built after 1981 in L'Aquila area) may be even better (Class E).

The proposed correlation between  $V$  and  $Q$  may be considered valid for masonry buildings, at least in Italy. In the case of other building types, e.g. in RC, the correlation should be verified/updated analogously from observed damage, starting from Eq. (8).

### 3.3 Formulation of the heuristic vulnerability model

In the previous sections the macroseismic vulnerability method was validated by the observed damage data collected in Da.D.O.. In particular, the general framework of EMS98 turned out to be very effective to describe the vulnerability of the different building types both in terms of progression of damage with the macroseismic intensity and of damage levels distribution. A simple refinement to the formulation has been proposed, in order to better calibrate the method with observed data.

Indeed, the macroseismic vulnerability method has the drawback of being formulated in terms of macroseismic intensity  $I$ , while seismic risk and scenario analyses usually adopt as input the  $PGA$  (or other physically based intensity measures). The conversion of the method was already proposed (Lagomarsino and Cattari 2014) by using  $I$ - $PGA$  correlation taken from literature. However, the dispersion of the available correlations (Murphy and O'Brien 1977; Guagenti and Petrini 1989; Margottini et al. 1992; Faccioli and Cauzzi 2006; Faenza and Michelini 2010) is huge, because derived in different countries and, sometimes, considering data from different earthquakes.

In this paper the conversion is made by fitting a new correlation with the shake maps of the events for which the observed damage was available. In particular the shake map of L'Aquila earthquake (2009) was used, because it is based on a significant number of records and on updated models; on the contrary, the shake map of the Irpinia earthquake (1980) was neglected due to some inconsistencies that have been detected in many towns with the reliable values of the assigned macroseismic intensity. The use of a correlation directly derived on the earthquake for which the damage data are available reduces the possibility of accumulation of errors. The Authors have named the method as "heuristic vulnerability model" because it combines, in a no rigorous and intuitive way, the general framework of the macroseismic method and the available damage and seismic input data.

Most of the  $I$ - $PGA$  correlations are formulated in this form:

$$\text{Log}(PGA) = aI + b \tag{11}$$

but may be transformed as follows:

$$PGA = c_1 c_2^{I-5} \tag{12}$$

where:

$$c_1 = 10^{5a-b} \quad c_2 = 10^a \tag{13}$$

are coefficient to be fitted from the available data; in particular,  $c_1$  represents the  $PGA$  for intensity  $I=5$ , while  $c_2$  is the factor of increase of  $PGA$  due to an increase of 1 of

the macroseismic intensity. Figure 11a shows the statistic values of the *PGA*, in locations with the same macroseismic intensity *I*, derived from the L'Aquila earthquake shake map (median values, 16% and 84% quantiles) and the linear least square regression; that allowed to provide the coefficients of Eq. (11). Figure 11b shows all the available data (grey bubbles), with the obtained correlation, compared with the above-mentioned correlations from the literature. As expected, the dispersion is huge but a general trend is evident, except for *I*=6: it is worth noting that the *PGA* values from the shake map have the ambition to take also into account of site effects, while the macroseismic intensity is associated to the whole urban centre (or, even to the municipality). Anyhow, the median correlation ( $c_1=0.05$  g,  $c_2=1.66$ ) is quite close to all the available correlations (except the one from Faenza and Michelini 2010), despite the huge dispersion.

The heuristic vulnerability model identifies any sub-type of masonry buildings (defined by a combination of attributes from the available inventory) by the vulnerability index *V*. By assuming the correlation of Eq. (12), it is possible to derive the median value  $PGA_{Dk}$  for the fragility curve of each damage level ( $k=1,\dots,5$ ), passing through the corresponding intensity  $I_{Dk}$ , given by Eq. (6) in the original macroseismic method; however, the latter have been here evaluated using the calibrated method, represented by Eq. (10). The following equation is derived for  $V \geq 0.32$ , as this heuristic vulnerability model is proposed for masonry buildings:

$$PGA_{Dk}(V, k) = c_1 c_2^{(I_{Dk}-5)} = c_1 c_2^{[6.7-3.45V+(0.9+2.8V)atanh(0.36k-1.08)]} \tag{14}$$

The complete fragility curve is directly obtained numerically, by using the eqns. (1), (10) and (12), but the trend is very well fitted by the lognormal cumulative distribution, by calibrating the values of the dispersion  $\beta_{Dk}$ . The dispersion implicitly results from: (i) the new calibrated macroseismic vulnerability curve; (ii) the binomial distribution of damage levels; (iii) the assumed *I*-*PGA* correlation (in particular through the parameter  $c_2$ ).

Figure 12 shows the fragility curves representative of the vulnerability classes A ( $V=1$ ) and C ( $V=0.6$ ). For each class, the best fitting is obtained by slightly different values of the dispersion for each damage level; however, the use of different values with the lognormal distribution leads to the intersection of the corresponding fragility curves

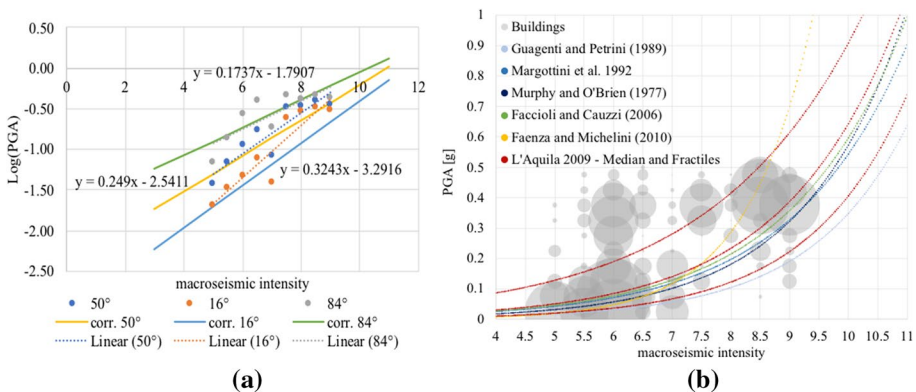


**Fig. 11** *I*-*PGA* correlations: **a** derivation from L'Aquila earthquake; **b** comparison with correlations from the literature (grey bubbles are proportional to the number of buildings in the corresponding PGA bin)

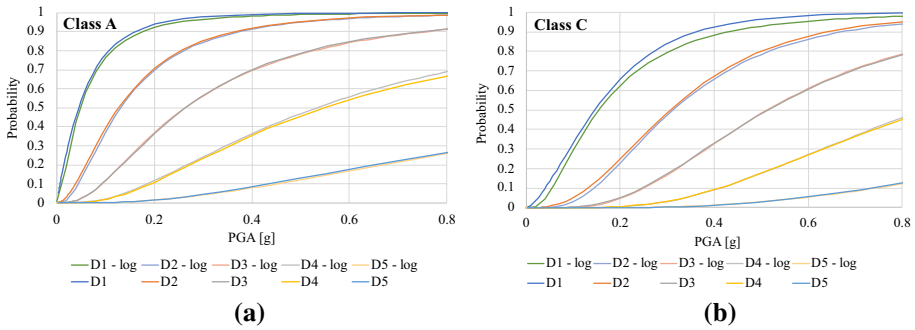


**Fig. 12** Fragility curves of the heuristic vulnerability model for the EMS98 Classes A and C

for low  $PGA$  values (when  $\beta_{Dk} < \beta_{Dk+1}$ ) or high  $PGA$  values (when  $\beta_{Dk} > \beta_{Dk+1}$ ). Even if these intersections may occur out of the significant range of  $PGA$  (the one used for the risk calculation by the convolution integral), it is better to assume an average constant value  $\beta_D$  of the dispersion for the all set of fragility curves ( $k = 1, \dots, 5$ ). On the contrary, the influence of  $V$  on the dispersion should be considered: this means that each vulnerability class has a proper dispersion.

A good fitting is provided by the following equation:

$$\beta_D(V, c_2) = 0.25c_2 - 0.16 + (0.73c_2 - 0.56)V \tag{15}$$

which may be simplified in the following, for the model derived from the L'Aquila shake map:

$$\beta_D(V) = 0.25 + 0.65V \tag{16}$$

Therefore, the heuristic vulnerability model for masonry buildings provides analytically the set of fragility curves of a set of buildings, classified by a proper taxonomy through the attribution of the specific vulnerability index  $V$  (or range of values), and assuming the proper  $I$ - $PGA$  correlation for the study area (in terms of the parameters  $c_1$ — $PGA$  for intensity  $I=5$ —and  $c_2$ —factor of increase of  $PGA$  due to an increase of 1 of the macroseismic intensity). The median values  $PGA_{Dk}$  for the different damage grades and the dispersion  $\beta_D$  (assumed constant for all damage levels) are given by eqns. (14) and (15).

For the six vulnerability classes of EMS98, the white values  $V_i$  ( $i = A, B, \dots, F$ ) of the vulnerability index have been assumed as reference (see Table 10). The classification of buildings only in terms of the masonry type (Fig. 2) implies that within the set there are buildings of different vulnerability class. Each subset is represented by the above-introduced fragility curves, while the behavior of the whole masonry type may be obtained through a combination of the response of the vulnerability classes that are present, weighted by a coefficient  $w_i$  ( $i = A, B, \dots, F$ ). The latter may be estimated from the table in Fig. 2 and by a specific knowledge of the buildings in the study area. As an alternative, one single set of fragility curves may be evaluated as representative for the whole masonry type. The median values  $PGA_{Dk}^*$  may be evaluated with Eq. (14) by considering the representative vulnerability index  $V^*$ , which may be evaluated as:

$$V^* = \sum_{i=A}^F w_i V_i \tag{17}$$

The dispersion should be increased with respect to the one related to a single value of the vulnerability index, given by Eq. (16), by considering two additional contributions due to:

- (1) The possible variation of values  $V$  in each vulnerability class (even out of the plausible range in Table 10, according to the fuzzy set theory—Lagomarsino and Giovinazzi 2006).
- (2) The variability of the median values of the  $PGA_{Dk}(V_i)$ , weighted by  $w_i$ , for involved vulnerability classes. It is worth remembering that the dispersion is referred to the logarithm of the  $PGA$ .

The first contribution may be evaluated by concentrating the variation of  $V$  in the class at the extremes of the plausible range. After simple mathematical steps the following formula is obtained:

$$\beta_1 = \begin{cases} 0.05 \log c_2 [3.45 - 2.8 \operatorname{arctanh}(0.36k - 1.08)] & \text{for } V \geq 0.32 \\ 0.3125 \log c_2 & \text{for } V < 0.32 \end{cases} \tag{18}$$

which is simplified, assuming the  $I$ - $PGA$  correlation from L'Aquila earthquake, as follows:

$$\beta_1 = \begin{cases} 0.088 [1 - 0.8 \operatorname{arctanh}(0.36k - 1.08)] & \text{for } V \geq 0.32 \\ 0.158 & \text{for } V < 0.32 \end{cases} \tag{19}$$

The second contribution may be evaluated as follows:

$$\beta_2 = \sqrt{\sum_{i=A}^F w_i [\log PGA_{Dk}(V_i)]^2 - \left[ \sum_{i=A}^F w_i \log PGA_{Dk}(V_i) \right]^2} \tag{20}$$

By assuming all these contributions as independent, the dispersion  $\beta^*$  of the whole masonry type is obtained as follows:

$$\beta^* = \sqrt{\sum_{i=A}^F w_i [\beta_D(V_i)]^2 + \beta_1^2 + \beta_2^2} \tag{21}$$

where the last two contributions depend both by the damage level  $k$ . As they decrease for the higher damage grades, the total dispersion decreases and the possibility of an intersection of the fragility curves for high values of  $PGA$  cannot be excluded and should be checked in the range adopted for the risk integration.

By way of example, the fragility curves for two masonry types are evaluated, by assuming a combination of the vulnerability classes coherently with EMS98 (Fig. 2):

- M2—simple stones masonry: most of the buildings are of vulnerability class B, but also some exceptional cases are of class A.
- M6—unreinforced with RC floors: most of the buildings are of vulnerability class C, but a significant percentage are of class B and some exceptional cases are of class D.

**Table 11** Parameters assumed to derive fragility curves for two masonry types

	Simple stones masonry			Unreinforced with RC floors			
	A	B	M2	B	C	D	M6
$w_i$	0.15	0.85	$V^*=0.83$	0.25	0.65	0.1	$V^*=0.63$
$V_i$	1	0.8		0.8	0.6	0.4	
$\beta_D$	0.90	0.77	$\beta_D^*=0.791$	0.77	0.64	0.51	$\beta_D^*=0.664$
$k$	$\beta_1$	$\beta_2$	$\beta^*$	$k$	$\beta_1$	$\beta_2$	$\beta^*$
1	0.152	0.217	<b>0.83</b>	1	0.152	0.348	<b>0.76</b>
2	0.115	0.163	<b>0.82</b>	2	0.115	0.261	<b>0.72</b>
3	0.088	0.125	<b>0.81</b>	3	0.088	0.200	<b>0.70</b>
4	0.061	0.087	<b>0.80</b>	4	0.061	0.139	<b>0.68</b>
5	0.024	0.033	<b>0.79</b>	5	0.024	0.053	<b>0.67</b>

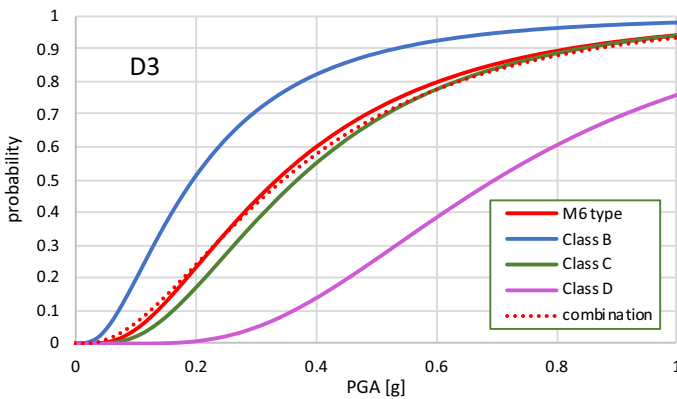


**Fig. 13** Fragility curve of damage level 3 for M6 type: comparison between the one obtained by the heuristic vulnerability model and those of the vulnerability classes relevant for M6 type

Table 11 shows the assumed weights  $w_i$  and the consequent parameters of the fragility curves. Regarding the dispersion, it emerges that the contribution of  $\beta_1$  is almost negligible, while that of  $\beta_2$  is more significant, in particular for M6 type that is formed by buildings of three different vulnerability classes. The resulting dispersion  $\beta^*$  is not constant but decreases for the highest damage levels: this implies intersections between fragility curves, but actually they do not occur for the *PGA* of interest. Figure 13 shows the fragility curve of damage level 3 for M6 type, obtained from the parameters in Table 11, compared with those of the vulnerability classes B, C and D, as well as the one obtained by a weighted combination of the latter (dotted line). Conceptually, the fragility curve obtained by the combination is the correct one but the definition of an accurate single lognormal curve is very helpful.



## 4 Risk assessment of the Italian masonry buildings

The risk assessment of the Italian masonry buildings was made by using the inventory of the residential buildings from the ISTAT census of 2001, which consists of information on the number of buildings, number of flats, flat surface and resident people, aggregated in each town by considering: the building material (masonry M and reinforced concrete RC), the age of construction and the number of stories. According to this classification, 15 sub-types of masonry buildings have been identified and named by the following tags: M/L-M-H/A1-A5 (masonry/number of stories/age of construction).

According to the heuristic vulnerability model, the vulnerability index characteristic of each building sub-type from ISTAT was obtained from a calibration with the observed damage in Da.D.O. (Sect. 3.2).

The risk calculation was made by the IRMA platform, developed by Eucentre coherently with the EMS98 framework (Borzi et al. 2018), through the implementation of the sets of fragility curves for the vulnerability classes and the definition of a building typology matrix, which identifies for the 15 ISTAT sub-types the percentage of buildings performing like each vulnerability class.

### 4.1 Vulnerability of the ISTAT sub-types of masonry buildings

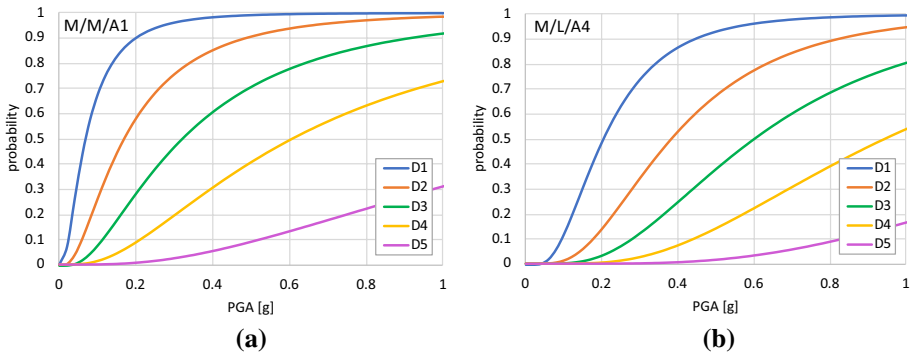
Although some differences have been noticed from the data processing of Irpinia and L'Aquila earthquakes (Sect. 3.2), at this stage of the research, the risk assessment is made without distinguishing the regional vulnerability (Masi et al. 2021), because data are not sufficient to have a clear picture all over Italy.

Figure 5b shows that the vulnerability that comes out from other regions/earthquake is between that resulting from the two earthquakes analysed in detail. Therefore, average values of the vulnerability index were assumed for the masonry buildings sub-types (Table 12). It is worth noting that mid-rise buildings result less vulnerable than the low-rise ones when built before 1945, probably because the latter are often very poor and rural while after the Second World War the engineered masonry buildings are more vulnerable if higher. As already mentioned, empirical data are not statistically robust for high-rise buildings: thus, the vulnerability index was estimated by analogy through an expert judgment, taking into consideration the values for the low and mid-rise ones.

Figure 14 shows the fragility curves for ISTAT sub-types M/M/A1 and M/L/A4, obtained by assuming the vulnerability index from Table 12 and by evaluating the median values from Eq. (14) and the dispersion by Eq. (21); the contribution of  $\beta_D$ —Eq. (16)—and  $\beta_I$ —Eq. (18)—is considered but that of  $\beta_2$  is neglected. Indeed, the ISTAT sub-types does not distinguish the masonry type but the dispersion is similar to that of a vulnerability

**Table 12** Vulnerability indexes representative of the ISTAT masonry sub-types

ISTAT sub-type	A1 (<1919)			A2 (1919–1945)			A3 (1946–1961)			A4 (1962–1981)			A5 (>1981)		
	L	M	H	L	M	H	L	M	H	L	M	H	L	M	H
V	0.92	0.88	0.98	0.82	0.76	0.88	0.68	0.70	0.74	0.52	0.56	0.60	0.4	0.42	0.44



**Fig. 14** Vulnerability curves from the heuristic vulnerability model for two of the ISTAT masonry sub-type: **a** mid-rise built before 1919 (M/M/A1); **b** low-rise built between 1962 and 1981 (M/L/A4)

class, because in the set there are buildings of the same age and height (the damage histogram resulted well approximated by a binomial distribution—Fig. 7).

## 4.2 Implementation of the developed fragility curves in the IRMA platform

The IRMA platform requires the set of fragility curves (for the 5 damage grades D1/2/3/4/5) for the vulnerability classes (A/B/C1/C2/D), allowing to implement different sets for different classes of height (L/M/H). The fragility of each ISTAT sub-type is provided by the exposure/vulnerability matrix where, for each sub-type (age and height—Table 12), the percentage of buildings that behave like each vulnerability class is given.

This approach is fully compatible with the EMS98 framework, which assumes that in each masonry type there are buildings of different vulnerability (Fig. 2). Therefore, it is also compatible with the proposed heuristic vulnerability model.

The first step is to assume set of fragility curves for the EMS98 vulnerability classes. To this end the mean values of the vulnerability index  $V$  in the plausible range have been assumed (Table 10) for all the classes of height. Indeed, it is not necessary to distinguish the fragility curves with the height, because the different vulnerability of each sub-type can be made by the exposure/vulnerability matrix. This distinction would be useful in case of an experimental evidence that the low-rise buildings are systematically better or worse than mid-rise buildings.

It is worth noting that IRMA platform distinguishes, within class C, two independent classes C1 and C2. This is due to the fact that in the literature, empirical methods usually make a direct association between vulnerability classes and macro-typologies of buildings: (A) poor masonry buildings; (B) good quality masonry buildings; (D) seismically designed RC buildings. In class C there are both the modern masonry buildings and the “gravitational” RC buildings; as the vulnerability curves may be not exactly the same, the two classes are distinguished by C1 and C2. The direct correlation between building types and vulnerability classes would be an oversimplification in case the ISTAT sub-types are adopted, therefore also the distinction between C1 and C2 is not useful. Anyhow, this paper deals only with masonry buildings, so class C1 is used and named C in the following.

The second step, that is the implementation of the exposure/vulnerability matrix, is straightforward by using the heuristic vulnerability model, because it is sufficient to

**Table 13** Parameters of the fragility curves for the vulnerability classes implemented in the IRMA platform

	$PGA_{D1}$ (g)	$PGA_{D2}$ (g)	$PGA_{D3}$ (g)	$PGA_{D4}$ (g)	$PGA_{D5}$ (g)	$\beta_D$
A	0.047	0.128	0.260	0.526	1.424	0.90
B	0.087	0.202	0.368	0.671	1.561	0.77
C	0.159	0.319	0.522	0.855	1.712	0.64
D	0.293	0.504	0.741	1.090	1.877	0.51

**Table 14** Percentage of vulnerability classes in each ISTAT masonry sub-types, compatible with the vulnerability index calibrated from Da.D.O. observed damage

ISTAT sub-type	A1 (< 1919)			A2 (1919–1945)			A3 (1946–1961)			A4 (1962–1981)			A5 (> 1981)		
	L	M	H	L	M	H	L	M	H	L	M	H	L	M	H
A	60	40	90	10		40									
B	40	60	10	90	80	60	40	50	70						
C					20		60	50	30	60	80	100		10	20
D										40	20		100	90	80

evaluate the weights  $w_r$ —Eq. (17)—in order to obtain the vulnerability index of each sub-type (Table 12).

Table 13 shows the fragility curves implemented in IRMA for the vulnerability classes A/B/C/D, assumed the same for all the building heights (L/M/H).

Table 14 shows the percentage of buildings in the different vulnerability classes, for the ISTAT masonry building sub-types; it gives a clear picture of how the vulnerability changes with the age of construction. It is worth noting that IRMA does not use a specific set of fragility curves for each sub-type, but it combines the performance of the vulnerability classes indicated in Table 14.

## 5 Results and discussion

This section illustrates the results achieved by the proposed heuristic vulnerability model thanks to its implementation in the IRMA platform. Firstly, the model has been validated by the observed damage and loss scenario after the L’Aquila earthquake (2009) (Sect. 4.1). Secondly, the seismic risk at national level has been evaluated, for masonry residential buildings, and discussed by comparing the results with the evidence of past data and another assessment available in the literature (Sect. 4.2).

### 5.1 Validation of real damage and loss scenarios

The shake maps of the main earthquakes in Italy in the last 40 years are implemented in the IRMA platform. Therefore, it is possible to simulate the damage scenarios, with the heuristic fragility curves and the vulnerability/exposure matrix for ISTAT sub-types, and validate them with the observed damage in Da.D.O. However, the validation of Irpinia scenario is

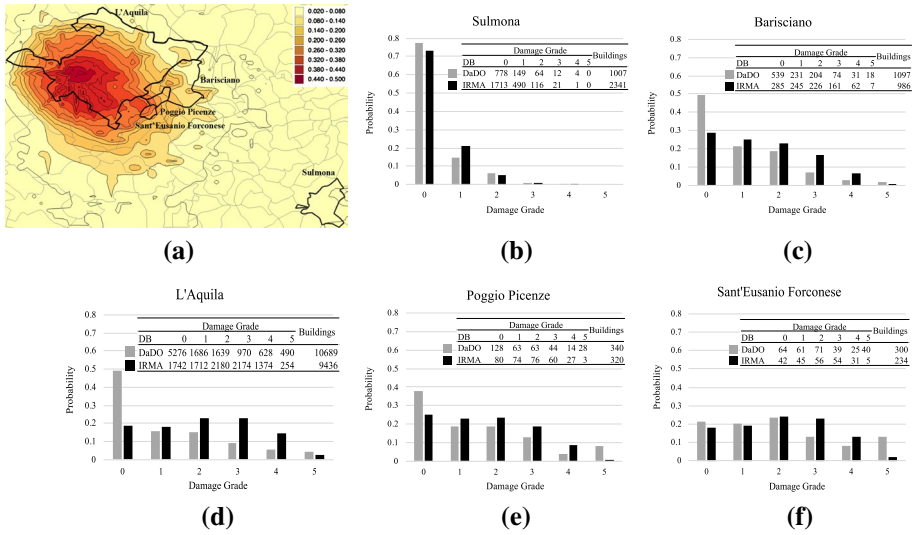


**Fig. 15** Estimated damage scenario: **a** shake map of L'Aquila earthquake (2009); **b–f** comparison of empirical and estimated damage histograms in different towns

**Table 15** Correlation between damage grades and repair cost (normalized to the rebuilt cost)

	D1 (%)	D2 (%)	D3 (%)	D4 (%)	D5 (%)
Lower bound	2	10	30	60	100
Upper bound	5	20	45	80	100

not possible, both because the shake map is not reliable (as already mentioned) and the building inventory (ISTAT 2001) does not reflect that hit by the 1980 earthquake (indeed, most of the buildings in the epicentral area collapsed and were rebuilt in the two following decades in RC).

On the contrary, L'Aquila scenario is a good test case, besides the problems related to the completeness of the survey, which is assured only in the epicentral area. Figure 15 shows: the shake map of the main event on April 6, 2009; and the comparison of damage level histograms, as empirically obtained from Da.D.O. and as evaluated by the heuristic vulnerability model through the IRMA platform, in five different locations with different distance from the epicenter. The results are in good agreement, except in the case of L'Aquila where the model overestimates the damage. Indeed, the presence of a high percentage of buildings with low or even no damage was already observed in Fig. 5 and may be related to a higher quality of the palaces in L'Aquila, compared with minor historical centers; in addition, also to the variability of the ground motion in the wide area of L'Aquila municipality (evident in Fig. 5a) could play a role. Indeed, in IRMA platform the building inventory is aggregated at municipality level and damage is evaluated with only one representative *PGA* value.

In order to have also a picture of the exposure (number of buildings and people involved in critical areas), it is necessary to use the consequence functions, which correlate the damage grades with monetary losses (Table 15) and aftermath on people and

**Table 16** Consequence functions in terms of percentage for each damage grade

Consequences		D1	D2	D3	D4	D5
Buildings	Unusable	0	0	60%	100%	0
	Collapsed	0	0	0	0	100%
People	Homeless	0	0	60%	100%	60%
	Seriously injured	0	0	0	5%	30%
	Deaths	0	0	0	1%	10%

**Table 17** Estimated losses and consequences after L'Aquila earthquake

	L'Aquila	Province of L'Aquila	Rome
Number of Buildings	8614	76,198	64,862
Blds unusable for a short period	1971	4449	205
Blds unusable for a long period	2506	4208	30
Collapsed buildings	217	299	0
Monetary loss (lowerbound)—M€	328	545	165
Monetary loss (upperbound)—M€	486	866	375
Population	67,844	295,130	739,175
Deaths	79	94	0
Seriously injured	293	352	2
Homeless	12,118	17,458	3829

buildings (Table 16). Regarding these correlations, few proposals may be found in the literature (Coburn and Spence 2002; Di Pasquale and Goretti 2001); herein, the assessment was made by using the default functions in the IRMA platform (Borzi et al. 2018; Faravelli et al. 2019). Table 17 reports the estimated losses in L'Aquila town and in the whole region affected by the seismic event, considering both the economic impact and the consequences to buildings and people. The results are in a good agreement with the actual ones (Dolce and Manfredi 2015; Dolce and Di Bucci 2017; Mannella et al. 2017). In particular:

- The number of victims is well estimated, considering that the one in the table ( $79 + 94 = 171$ ) refers only to masonry buildings (the actual number was 308, including RC buildings).
- The actual number of collapsed buildings were around 250.
- The homeless were initially 53,968, but they reduced to 32,008 after 18 months (a number compatible to that estimated:  $12,118 + 17,458 = 29,576$ ).
- In L'Aquila and the surrounding area, the residential buildings unusable for a short period were 3.954, while those unusable (requiring heavy reconstruction) were 6.906 (estimated values are  $1971 + 4449 = 6420$  and  $2506 + 4208 = 6714$ , respectively).
- The release of public funds related to residential buildings was about 2600 M€, including RC buildings and costs for the people assistance, an amount that is compatible with the range of monetary losses estimated through two different consequence functions (Table 16) (lowerbound:  $328 + 545 = 873$  M€; upperbound:  $486 + 866 = 1352$  M€).

Regarding last issue, the high uncertainties inherent in the table that correlates damage level to the cost of repair, normalized by the rebuilt cost is well known.

Table 17 also contains the estimated consequences in the city of Rome. This check was really important because fragility curves are usually calibrated for medium to high levels of the seismic intensity but may provide an overestimation of the damage for low values of PGA. The shakemap of L'Aquila main shock, implemented in IRMA, provides in Rome this seismic input:  $PGA=0.015$  g. Rome is a big city and so even in the case of a very low probability of damage occurrence, the total consequences may result significant. Although no information about buildings in Rome unusable for a long period have been recorded, for sure very vulnerable buildings suffered some damage (and few churches and palaces were closed); anyhow, 30 buildings over 64,862 is a negligible percentage 0.5‰ and below a certain threshold this calculation becomes meaningless.

## 5.2 Damage and loss assessment at national scale

The damage and loss assessment of masonry buildings in Italy was made by considering the probabilistic seismic hazard assessment MPS04 (Stucchi et al. 2004). The IRMA platform allows to evaluate a conditional scenario, that shows the damage and consequent losses due to the intensity corresponding, in each location, to the earthquake that has a given annual probability of occurrence (or return period). Considering the hypothetical occurrence all over the country of the  $PGA$  for a return period of 475 years (on soil type B), Fig. 16a shows the scenario of the mean damage grade of masonry buildings in each municipality, obtained by Eq. (2) by using the damage histogram that collects the masonry buildings of all ISTAT sub-types. It is worth noting that the damage distribution associated to this mean damage grade is not binomial, but this parameter is in any case more representative than a single damage level. This scenario gives a clear picture of the risk

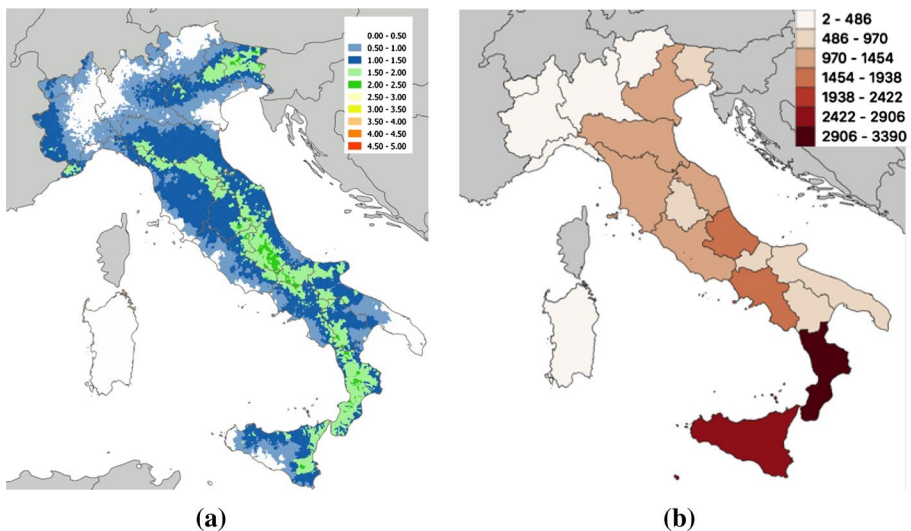


**Fig. 16** Seismic risk scenario conditioned to 475 years of return period (on soil type B): **a** mean damage grade; **b** number of collapsed buildings

distribution in Italy because it depends not only by the seismic hazard but also by the vulnerability in any municipality (distribution of sub-types, in terms of age of construction and height of the buildings).

Always with reference to the seismic hazard with return period of 475 years on soil type B, Fig. 16b shows, as an example, the number of masonry buildings that are prone to collapse; results are aggregated at regional level, because the representation at municipality level would be not effective.

The seismic risk assessment at national scale is better represented by unconditional scenarios, made by the fully probabilistic convolution integral, which takes into account the contribution of all possible earthquakes, each one with different intensity and probability of occurrence. The result is the probability of occurrence of a given consequence, computed in a reference period of time (e.g. annual or in 50 years). IRMA platform implements OpenQuake, a calculation engine developed by Global Earthquake Model (GEM) (<http://www.globalquakemodel.org>), for the numerical integration of risk, using the MPS04 hazard and the set of fragility curves implemented by the user. The integration starts from a low value of the *PGA* (0.03 g), which is considered a lower threshold for the onset of damage; it is worth noting that the probability of occurrence of this value is extrapolated from the point of MPS04 and that fragility curves are not validated below it.

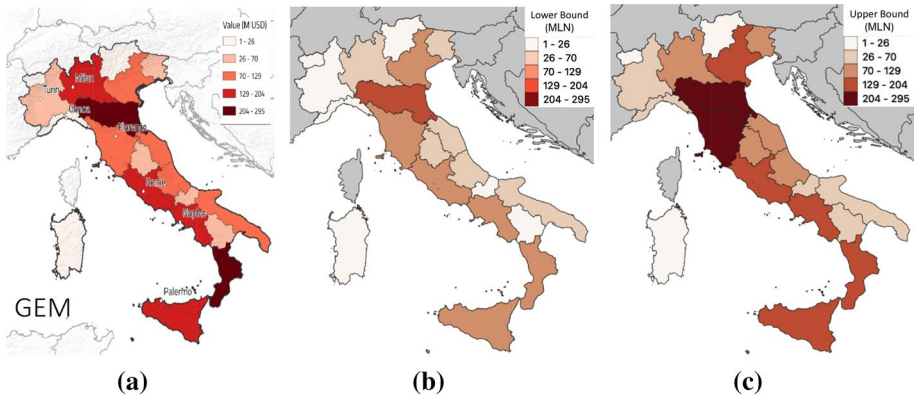
The results obtained by the heuristic vulnerability model are summarized in Table 18, under the alternative hypothesis of soil type A or B (at present, a map of soil types along the country is not implemented in IRMA and it is foreseen that the actual scenario is between these two). The complete validation of all these outcomes is not easy but some of them looks fine: (i) the number of deaths in Italy in the last 50 years (from Belice earthquake in 1968) has been 5.000, most of them in masonry buildings; (ii) the refunds paid by the Italian Civil Protection Department for the repair of damaged buildings amount on average to 2.500 M€/year.

Figure 17 shows the mean annual monetary loss: the assessment made by GEM Foundation (Silva et al. 2018, <https://downloads.openquake.org/countryprofiles/ITA.pdf>) for all residential buildings (Fig. 17a) is compared with costs evaluated by the heuristic vulnerability model with the lower and upper bound correlation between damage levels and cost ratio (in the case of soil type A). Data are aggregated at regional level, in order to be compatible with the format of GEM; costs are higher in the region with the highest seismic hazard (Calabria) but also where the exposure is higher (e.g. Emilia Romagna, Lazio,

**Table 18** Estimated mean annual (except indicated) losses and consequences of URM buildings in Italy

	Soil type A	Soil type B
Number of masonry buildings	7,899,972	
Blds unusable for a short period	8200 (0.96‰)	12,731 (1.61‰)
Blds unusable for a long period	3784 (0.43‰)	5899 (0.75‰)
Collapsed buildings	168	243
Monetary loss (lowerbound)—M€	1074	1668
Monetary loss (upperbound)—M€	2074	3220
Population	27,966,377	
Homeless	35,539	55,642
Seriously injured	294	445
Deaths (1 year)	77	116
Deaths (50 years)	3848	5750





**Fig. 17** Mean annual monetary loss (on soil type A): **a** GEM map ( source: <https://downloads.openquake.org/countryprofiles/ITA.pdf>); **b** and **c** lower and upper bound obtained from the proposed model (Table 15)

Campania and Lombardia). In order to compare the GEM scenario with the Authors’ range of estimates, Table 19 shows, at regional scale, if GEM is: equal to the lower (L), equal to the upper (U), higher than the upper (U<sup>+</sup>) or, the three are coincident (=). It emerges that, over 20 regions, GEM is 9 times comparable with the upperbound, and 3 times even higher, while only 5 times is similar to the lowerbound. It is worth noting the GEM esti-

**Table 19** Comparison of the mean annual monetary loss, at regional scale, estimated by GEM with the lower and upper bounds from the proposed model (for colors refer to legend in Fig. 17); last row indicates if GEM is equal to the lower (L) or the upper (U), or it is higher than the upper (U<sup>+</sup>) or the three are equal (=)

	Abruzzo	Basilicata	Calabria	Campania	Emilia Romagna	Friuli V. G.	Lazio	Liguria	Lombardia	Marche	Molise	Piemonte	Puglia	Sardegna	Sicilia	Toscana	Trentino Alto Adige	Umbria	Valle d’Aostia	Veneto	
Lower																					
GEM																					
Upper																					
	U	U	U <sup>+</sup>	U	U	L	U	L	U <sup>+</sup>	U	U	U	U <sup>+</sup>	=	U	L	=	L	=	L	

mate also includes RC buildings, which contribute less to the monetary loss because they are, on average, less vulnerable; therefore, the two estimates may be considered overall consistent.

## 6 Conclusions

The first important outcome of the paper is the calibration of the macroseismic vulnerability model originally proposed in Lagomarsino and Giovinazzi (2006) by means of a large database of observed vulnerability (Da.D.O.). Characteristic values of the vulnerability index have been associated to the vulnerability classes proposed in the EMS98 and to



masonry buildings sub-types, classified through the age of construction and the number of stories, while fragility curves in terms of intensity are derived analytically.

Then, a new model, named heuristic vulnerability model, has been formulated in terms of *PGA*, by means of a macroseismic intensity-*PGA* correlation, directly obtained from the shake map of the L'Aquila earthquake (2009). The classification of masonry buildings is based on the material types, according to the correlation with the vulnerability classes proposed in the EMS98, and to other specific features, in order to obtain a representative vulnerability index  $V^*$ . The set of lognormal fragility curves is obtained by evaluating analytically the median values of  $PGA_{Dk}$  for the different damage grades, as a function of the vulnerability index  $V^*$  and the corresponding dispersions  $\beta^*$  taking into account through proper weights the composition of the building subtypes in terms of vulnerability classes.

The heuristic vulnerability model has been implemented in the IRMA platform, which allowed a validation through the observed damage scenario after the L'Aquila 2009 earthquake. Finally, the model was used for the seismic risk assessment of masonry residential buildings in Italy. Monetary losses and consequences to buildings and people have been evaluated through consequence functions taken from literature. Results at regional and national scale have been compared with some available information on the impacts of past events in Italy, showing the good performance of the model.

**Acknowledgements** The results were achieved in the national research project ReLUIS-DPC 2018 ([www.reluis.it](http://www.reluis.it)), supported by the Italian Civil Protection Agency. The Authors thank Sabrina Vignolo for the support in processing the data of Da.D.O. database.

**Funding** Open access funding provided by Università degli Studi di Genova within the CRUI-CARE Agreement.

**Open Access** This article is licensed under a Creative Commons Attribution 4.0 International License, which permits use, sharing, adaptation, distribution and reproduction in any medium or format, as long as you give appropriate credit to the original author(s) and the source, provide a link to the Creative Commons licence, and indicate if changes were made. The images or other third party material in this article are included in the article's Creative Commons licence, unless indicated otherwise in a credit line to the material. If material is not included in the article's Creative Commons licence and your intended use is not permitted by statutory regulation or exceeds the permitted use, you will need to obtain permission directly from the copyright holder. To view a copy of this licence, visit <http://creativecommons.org/licenses/by/4.0/>.

## References

- ASCE/SEI 41-13 (2014) Seismic evaluation and retrofit of existing buildings. American Society of Civil Engineers, Reston, VA, ISBN 978-0-7844-7791-5
- Baggio C, Bernardini A, Colozza R, Corazza L, Della Bella M, Di Pasquale G, Dolce M, Goretta A, Martinelli A, Orsini G, Papa F, Zuccaro G (2002) Manuale per la compilazione della scheda di 1° livello di rilevamento del danno, pronto intervento e agibilità per edifici ordinari nell'emergenza post-sismica (AeDES). Department of Civil Protection, Rome (**in Italian**)
- Bernardini A, Lagomarsino S, Mannella A, Martinelli A, Milano L, Parodi S (2011) Forecasting seismic damage scenarios of residential buildings from rough inventories: a case-study in the Abruzzo Region (Italy). Proc IMech E Part OJ Risk Reliab 224:279–296
- Bertelli S, Rossetto T, Ioannou I (2018) Derivation of empirical fragility functions from the 2009 Aquila earthquake. In: Proceedings of the 16th European conference on earthquake engineering, Thessaloniki, pp 1–12
- Borzi B, Crowley H, Pinho R (2008) Simplified pushover-based earthquake loss assessment (SP-BELA) method for masonry buildings. Int J Archit Herit 2(4):353–376

- Borzi B, Faravelli M, Onida M, Polli D, Quaroni D, Pagano M, Di Meo A (2018) Irma platform (Italian Risk MAPs). In: Proceedings of the 37th national conference GNGTS. 19–21 November 2018, Bologna, Italy (in Italian)
- Castillo A, Lopez-Almansa F, Pujades LG (2011) Seismic risk analysis of urban non-engineered buildings: application to an informal settlement in Merida, Venezuela. *Nat Hazards* 59(2):891–916
- CEN (2005) Eurocode 8: design of structures for earthquake resistance—part 3: assessment and retrofitting of buildings. EN1998–3:2005. Comité Européen de Normalisation, Brussels
- Cherif SE, Chourak M, Abed M, Pujades L (2017) Seismic risk in the city of Al Hoceima (north of Morocco) using the vulnerability index method applied in Risk-UE project. *Nat Hazards* 85(1):329–347
- Coburn A, Spence R (2002) *Earthquake protection*, 2nd edn. Wiley
- Cornell CA, Krawinkler H (2000) Progress and challenges in seismic performance assessment. *PEER News*
- Cosenza E, Del Vecchio C, Di Ludovico M, Dolce M, Moroni M, Prota A, Renzi E (2018) The Italian guidelines for seismic risk classification of constructions: technical principles and validation. *Bull Earthq Eng* 16(12):5905–5935
- Del Gaudio C, De Martino G, Di Ludovico M, Manfredi G, Prota A, Ricci P, Verderame GM (2017) Empirical fragility curves from damage data on RC buildings after the 2009 L'Aquila earthquake. *Bull Earthq Eng* 15:1425–1450
- Del Gaudio C, Di Ludovico M, Magenes G, Penna A, Polese M, Prota A, Ricci P, Rosti A, Rota M, Verderame GM (2019a) A procedure for seismic risk assessment of Italian RC buildings. *COMPdyn Proc* 1:1759–1769
- Del Gaudio C, De Martino G, Di Ludovico M, Manfredi G, Prota A, Ricci P, Verderame GM (2019b) Empirical fragility curves for masonry buildings after the 2009 L'Aquila, Italy, earthquake. *Bull Earthq Eng* 17(11):6301–6330
- Dolce M, Manfredi G (2015) Libro bianco sulla ricostruzione privata fuori dai centri storici nei comuni colpiti dal sisma dell'Abruzzo del 6 aprile 2009. ReLUIS (in Italian)
- Dolce M, Di Bucci D (2017) Comparing recent Italian earthquakes. *Bull Earthq Eng* 15:497–533. <https://doi.org/10.1007/s10518-015-9773-7>
- Dolce M, Speranza E, Giordano F, Borzi B, Bocchi F, Conte C, Di Meo A, Faravelli M, Pascale V (2017) Da.D.O.—A web-based tool for analyzing and comparing post-earthquake damage database relevant to national seismic events since 1976. In: Proceedings of the 17th Italian conference on earthquake engineering, Pistoia (Italy)
- Dolce M, Speranza E, Giordano F, Borzi B, Bocchi F, Conte C, Di Meo A, Faravelli M, Pascale V (2019) Observed damage database of past Italian earthquakes the Da.D.O. Webgis. *Bollettino di Geofisica Teorica e Applicata* 60(2):141–164
- Dolce M, Prota A (2020) Foreword to the special issue on IRMA project. *Bull Earthq Eng* (this special issue)
- Masi A, Lagomarsino S, Dolce M, Manfredi V, Ottonelli D (2021) Towards the updated Italian seismic risk assessment: exposure and vulnerability modelling. *Bull Earthq Eng*. <https://doi.org/10.1007/s10518-021-01065-5>
- Donà M, Carpanese P, Follador V, da Porto F (2019) Derivation of mechanical fragility curves for macro-typologies of Italian masonry buildings. *COMPdyn Proc* 1:1691–1706
- Faccioli E, Cauzzi C (2006) Macro seismic intensities for seismic scenarios estimated from instrumentally based correlations. In: Proceedings of the first European conference on earthquake engineering and seismology, Geneva, Switzerland, September 3–8, 2006, CD-ROM
- Faenza L, Michelini A (2010) Regression analysis of MCS intensity and ground motion parameters in Italy and its application in ShakeMap. *Geophys J Int* 180(3):1138–1152. <https://doi.org/10.1111/j.1365-246X.2009.04467.x>
- Faravelli M, Polli D, Quaroni D, Onida M, Pagano M, Meo AD, Borzi B (2019) Italian platform for seismic risk and damage scenario evaluation. *COMPdyn Proc* 1:1630–1640
- Grunthal G (1998) European Macroseismic Scale. *Chaiers du Centre Européen de Géodynamique et de Séismologie*, Vol. 15, Luxembourg
- Guagenti E, Petrini V (1989) Il caso delle vecchie costruzioni: verso una nuova legge danni-intensità. In: Proceedings of 4th Italian conference on earthquake engineering, Milano, Vol. I, pp. 145–153 (in Italian)
- HAZUS (1999) *Earthquake loss estimation methodology—technical and user manuals*. Federal Emergency Management Agency
- ISTAT, Italian National Institute of Statistics (2001) 14°C censimento della popolazione—Istruzioni per il rilevatore, Rome (in Italian)
- Italian Civil Protection Department (2018) National Risk Assessment 2018. Overview of the potential major disasters in Italy. Updated December 2018

- Klir GJ, Yuan B (1995) Fuzzy sets and fuzzy logic. Theory and applications, Prentice Hall, New Jersey
- Jaiswal K, Wald D, D'Ayala D (2011) Developing empirical collapse fragility functions for global building types. *Earthq Spectra* 27(3):775–795
- Lagomarsino S, Giovinazzi S (2006) Macroseismic and mechanical models for the vulnerability assessment of current buildings. *Bull Earthq Eng* 4(4):445–463
- Lagomarsino S, Cattari S (2013) Seismic vulnerability of existing buildings: observational and mechanical approaches for application in urban areas. In: Gueguen P (ed) *Seismic vulnerability of structures*. ISTE Ltd and Wiley, pp 1–62
- Lagomarsino S, Cattari S (2014) Fragility functions of masonry buildings. In: Pitilakis K, Crowley H, Kaynia AM (eds) *SYNER-G: typology definition and fragility functions for physical elements at seismic risk: elements at seismic risk, geotechnical, geological and earthquake engineering*. Springer
- Lagomarsino S, Cattari S (2015) PERPETUATE guidelines for seismic performance-based assessment of cultural heritage masonry structures. *Bull Earthq Eng* 13(1):13–47. <https://doi.org/10.1007/s10518-014-9674-1>
- Lestuzzi P, Podestà S, Luchini C, Garofano A, Kazantzidou-Firtinidou D, Bozzano C, Bischof P, Haffter A, Rouiller JD (2016) Seismic vulnerability assessment at urban scale for two typical Swiss cities using Risk-UE methodology. *Nat Hazards* 84(1):249–269
- Maio R, Ferreira TM, Vicente R (2018) A critical discussion on the earthquake risk mitigation of urban cultural heritage assets. *Int J Disaster Risk Reduc* 27:293
- Mannella A, Di Ludovico M, Sabino A, Prota A, Dolce M, Manfredi G (2017) Analysis of the population assistance and returning home in the reconstruction process of the 2009 L'Aquila earthquake. *Sustainability* 9:1395
- Margottini C, Molin D, Narcisi B, Serva L (1992) Intensity versus ground motion: a new approach using Italian data. *Eng Geol* 33:45–48
- Moehle JP, Deirelein GG (2004) A framework methodology for performance-based earthquake engineering. In: *Proceedings of the 13th world conference on earthquake engineering*, Paper 679
- Murphy JR, O'Brien LJ (1977) The correlation of peak ground acceleration amplitude with seismic intensity and other physical parameters. *Bull Seismol Soc Am* 67:877–915
- Neves F, Costa A, Vicente R, Oliveira CS, Varum H (2012) Seismic vulnerability assessment and characterization of the buildings on Fail Island, Azores. *Bull Earthq Eng* 10(1):27–44
- Porter KA (2003) An overview of PEER's performance-based earthquake engineering methodology. In: *Proceedings of the ninth international conference on applications of statistics and probability in engineering*, San Francisco, USA
- Rossetto T, D'Ayala D, Ioannou I, Meslem A, Pitilakis K, Crowley H, Kaynia AM (2014) SYNER-G: typology definition and fragility functions for physical elements at seismic risk. *Geotechnical geological and earthquake engineering*, vol 27. Springer
- Rosti A, Rota M, Magenes G, Penna A (2019) A procedure for seismic risk assessment of Italian masonry buildings. *COMPdyn Proc* 1:1653–1663
- Rota M, Penna A, Strobbia CL (2008) Processing Italian damage data to derive typological fragility curves. *Soil Dyn Earthq Eng* 28(10–11):933–947
- Silva V, Amo-Oduro D, Calderon A, Dabbeek J, Despotaki V, Martins L, Rao A, Simionato M, Viganò D, Yepes-Estrada C, Acevedo A, Crowley H, Horspool N, Jaiswal K, Journeay M, Pittore M (2018) Global Earthquake Model (GEM). *Seismic Risk Map* (version 2018.1). <https://doi.org/10.13117/GEMGLOBAL-SEISMIC-RISK-MAP-2018>
- Stucchi M, Meletti C, Montaldo V, Akinci A, Faccioli E, Gasperini P, Malagnini L, Valensise G (2004) Italian seismic hazard map MPS04. ING—Istituto Nazionale di Geofisica e Vulcanologia (in Italian)